University of Alberta

Influence of State Alternations and Cholinergic Manipulations on the Synaptic Excitability of Hippocampal Pathways

By

Kurt Peter Schall

A thesis submitted to the Faculty of Graduate Studies and Research in partial fulfillment of the requirements for the degree of Master of Science

Department of Psychology

Edmonton, Alberta

Spring, 2008

Your file Votre référence
ISBN: 978-0-494-45882-2
Our file Notre référence
ISBN: 978-0-494-45882-2

Abstract

The operation of the hippocampus (HPC) is crucial for declarative memory formation and consolidation. HPC processing has been linked to its network activities, specifically the theta rhythm and slow oscillation (SO). We compared the synaptic responsiveness of various HPC pathways in urethane anesthetized rats across different spontaneous or cholinergically evoked states. In CA1 (the output station of the HPC), synaptic inputs from CA3 and the temporal ammonic pathway were more responsive during SO. In the dentate gyrus (the input station of the HPC) the medial and lateral perforant pathways showed opposing patterns of modulation with the medial component enhanced during theta. Furthermore, we also observed additional modulation within both the theta and SO rhythms, dependent on when stimulation occurred in the phase of the ongoing cycle. These results demonstrate that the network state of the HPC plays a major role in neural processing and support the notion that theta and SO could be differentially involved in memory encoding and consolidation, respectively.

Table of Contents

List of Figures

Chapter 1: Introduction

Imagine you are in a room when a stranger walks in and begins a conversation with you. The conversation is normal but enjoyable and as the person leaves the room you think about how you were glad to have met them. Then, five minutes later the same person walks back into the room and begins to talk to you but you have no idea who they are or any recollection that you have met them before. Later in the day you look at the clock and notice it is noon so you decide to have lunch. A half an hour later you look at the clock again and forgetting that you have recently ate, assume that you must be hungry and eat again. In the afternoon you recall a fond childhood memory of your father and start to think about going to visit him. Someone informs you that your father had passed away a few years ago and that you have been told many times but you just do not remember.

This is a limited description of the life of the neurological patient HM, who underwent surgery in the 1950's to remove significant portions of his medial temporal lobe (MTL) in both hemispheres as a desperate attempt to combat an increasingly debilitating epilepsy condition unresponsive to traditional treatment. Although the surgery was successful in alleviating HM's seizures, it had the unpredicted and devastating side effect of causing a form of anterograde amnesia (Scoville and Milner 1957; Corkin 1984). Anterograde amnesia is characterized by the inability of an individual to learn new information in the period following the onset of a brain injury or trauma. The surgery also appeared to cause a mild case of temporally graded retrograde amnesia, where memories just prior to the surgery were lost but older memories formed before a certain time point remained stable (Corkin 1984; Eichenbaum 2002). Based on these

observations it was speculated that structures in the MTL were necessary for the formation and temporary storage of memories but not required for their eventual permanent storage.

In contrast to the deficits endured by HM, it is also interesting to note the abilities that were not affected by the surgery. Despite the removal of a rather large portion of the brain, other cognitive functions such as perception, reasoning and intelligence remained stable as compared before and after his operation. HM also performed as well as controls on tasks measuring short-term memory (STM) in which subjects are required to remember a few items for a period of 30 seconds or less. In addition, studying HM's performance on a variety of memory tasks lead to the distinction of different memory classes or systems such as declarative and procedural memory. Declarative memory refers to memories that require a conscious effort during recall such as general facts and personal experiences. Procedural memory in contrast refers to memories that are formed implicitly like the unconscious improvement of a motor skill over time. Although HM was completely unable to form new declarative memories he still showed improvement on procedural memory tasks (Eichenbaum 2002).

The Hippocampus and Declarative Memory

Although HM's operation was not isolated to the removal of the hippocampus (HPC), it was the structure that received the most damage and became associated with the pattern of impairment observed in HM (Corkin et al. 1997). Additional human case studies of individuals with brain damage similar to but more specific than HM support the idea that damage to the HPC is responsible for deficits in declarative memory (Zola-Morgan et al.

1986; Stefanacci et al. 2000). In addition, a number of studies have shown that HPC lesions produce a deficit of recognition memory in monkeys (Mahut et al. 1981; Squire 1992 (review); Alvarez et al. 1995; Zola et al. 2000) as well as disrupt spatial and contextual memory in rats, believed to be comparable to declarative memory in humans (Morris et al. 1982; Clark et al. 2001; Winocur et al. 2001; Eichenbaum 2002). Although lesioning the HPC is sufficient to cause a deficit in memory, it has also been shown that increasing the lesion area to cortical or MTL structures forming connections with the HPC, such as the entorhinal cortex (EC), increase the degree of impairment (Jarrard et al. 1986; Alvarez et al. 1995). Therefore it has become a widely accepted fact that the MTL is responsible for declarative memory processing with the hippocampus playing a cornerstone role. The current view speculates that the HPC, through supporting structures in the MTL, receives highly processed information from the neocortex to form a new memory but over time sends the memory back to the neocortex for long-term storage through the process of consolidation.

Linking a brain structure or area to a particular process is an interesting and important step in its understanding but it does not provide a complete or final explanation. Knowing that the HPC is involved in memory formation is not the same as understanding what the HPC does and how this allows memories to be formed in the brain. This type of knowledge becomes especially important in the context of identifying normal memory processes in comparison to pathologies, ultimately having implications in addressing memory impairments. Therefore a great deal of effort in memory research is focused on the neurophysiological properties of the HPC and how they may relate to the established behavioral correlates of memory. Several variables can be suggested as obvious

influences on the way the hippocampus operates including extrinsic connections, internal organization, spontaneous network activity and synaptic plasticity.

Connections and Structure of the Hippocampus

As mentioned previously the HPC receives an input of highly processed information from the neocortex (Figure 1-1). Axons from the sensory associative areas of the cortex first synapse onto neurons of the superficial layers of the EC (Witter et al. 2000). The EC then projects a set of fibers known as the perforant path (PP) to the HPC (Amaral 2007). The PP has been subdivided into two separate components, the medial perforant path (MPP) and lateral perforant path (LPP), based on differences in anatomy, synaptic activity and neuropharmacology (McNaughton and Barnes 1977; McNaughton 1980; Fredens et al. 1984; Dahl and Sarvey 1989; Pang et al. 1993). Information is then processed in the HPC before it is sent back through the deep layers of the EC to the same sensory areas of the cortex that it originated from (Rolls 2000; Witter et al. 2000).

This cortical-hippocampal-cortical loop makes up the main processing circuit of the HPC. The nature of this circuit lends itself to the conceptualization a system whereby information could be sent to the HPC to be formed into memories and then subsequently returned to the originating cortical areas for long term store. It also suggests a pivotal role for the hippocampus in the formation and consolidation of declarative memories as it is the last structure to process the information before it is relayed back. As sensory information is initially processed by the cortex it becomes widely dispersed to various sensory regions separated by considerable distances across the cortical surface. This leads to a potential problem as to how the individual aspects of an experience are

integrated in a complete and meaningful way. The answer could lie in the convergence of these segregated components to a single structure, like the HPC, which could then process and integrate the individual streams into a higher level representation. Once the information has been integrated in this fashion it could then be sent back to the appropriate regions for permanent storage and potentially quicker accessibility during subsequent presentations of the same stimuli.

Within the HPC itself exists a number of differentiated regions containing subsets of neurons connected by major fibre tracts that transfer information across the HPC in a predominantly unidirectional flow (Figure 1-1). Information first enters the HPC via the PP which synapses on the dentate gyrus (DG) (Witter et al. 2000). In addition, a third branch of the PP, known as the temporal ammonic pathway (TA), has been identified and forms a direct connection to area CA1 of the HPC. A major fiber tract, known as the mossy fibers, emerges from the DG and synapse on area CA3 of the HPC (Amaral 2007). From CA3 a group of axons designated as the Schaffer Collaterals, connects to area CA1 (Amaral 2007). Area CA3 also send axons across the midline (called commissural fibres) that connects to the contra-lateral CA1 region. Area CA1 is the source of major output from the HPC and send projections through a structure called the subiculum to the deep layers of the EC (Rolls 2000). Although the trisynaptic pathway between the DG, CA3 and CA1 make up the primary flow of information through the HPC, there are several connections entering, leaving and within the HPC that skip over certain areas or flow in the opposite direction. This complicated network of connections gives the HPC a large degree of potential processing power.

Activity of the Hippocampus

In addition to studying the role that extrinsic and intrinsic connections play in the way information is processed in the HPC, researchers have also looked at how patterns of coordinated activity observed in the HPC are potentially related to memory functions. EEG recordings in the HPC taken from animals during awake behavior, sleep and anesthesia have revealed that the neural network of the HPC spontaneously alternates between the various activity states consisting of the theta rhythm, large amplitude irregular activity (LIA) (Vanderwolf 1969) and the recently discovered slow oscillation (SO) (Wolansky et al. 2006). These patterns of activity are differentiated based on their characteristic properties, are correlated with various behaviors and are proposed to underlie separate functions in the HPC.

The hippocampal theta rhythm is a relatively large amplitude, synchronous pattern of activity characterized by a frequency bandwidth of between 3 and 12 Hz (Bland 1986). However the theta rhythm is recognized as containing two subtypes. Type 1 theta has a bandwidth of 7 to 12 Hz and is not influenced by cholinergic manipulation while type 2 theta occurs between the frequencies of 3 to 7 Hz and is susceptible to cholinergic modulation (Bland 1986). Type 1 theta is correlated with the occurrence of movement (sometimes referred to as voluntary movements) such as walking, running and jumping, with the theta frequency being positively correlated with the speed or intensity of the movement in a rough fashion (Vanderwolf 1969; Morris 1976). Type 2 theta is correlated with presentation of sensory stimulation in the absence of movement and has therefore been linked to acts of memory and information encoding (Bland 1986). Type 2 theta is also observable during periods of REM sleep. Experiments have shown that

application of cholinergic antagonists, which disrupt type 2 theta, results in decreased performance on memory tests (Givens and Olton 1990; Andersen et al. 2002) but application of an agonist, which conversely promotes type 2 theta, increases performance (Haroutunian et al. 1985; Eidi et al. 2003). Because of its associated role with memory function the remaining discussion will focus on type 2 theta which will from this point on simply be referred to as theta.

Traditionally when the EEG recordings from the HPC of an animal was not showing theta, the resulting activity was classified as LIA. LIA as its name implies is state of irregular activity with no clear peak frequencies and a complete lack of synchrony or rhythmicity. LIA is correlated with alert immobility, behaviors such as grooming and eating, and periods of non REM sleep (Bland 1986).

Recently, a novel state of activity, the slow oscillation (SO), was discovered to occur in the hippocampus during periods of non REM sleep and under urethane anesthesia (Wolansky et al. 2006). SO is a very large amplitude, synchronous state of activity centered at a frequency of 1 Hz, very similar to (as well as correlated with) the slow rhythm present in the neocortex (Wolansky et al. 2006). The SO has been proposed as a mechanism to promote synchronization between the HPC and the neocortex allowing for a means of synaptic plasticity and information flow between the two that would be required for memory consolidation. Interestingly, studies have shown that the amount of slow wave sleep but not REM sleep is positively correlated with increased declarative memory consolidation (Fowler et al. 1973; Plihal and Born 1997; Takashima et al. 2006) while manipulations administered during slow wave sleep after a learning session has been shown to enhance consolidation (Rasch et al. 2007).

Synaptic Events in the Hippocampus

The existence of varying patterns of activity in the HPC and their assumed differential roles in the overall production of declarative memories is likely linked to their relationship with synaptic plasticity. The earliest speculation about a brain mechanism responsible for a memory has always been centered on the theory of synaptic changes between two or more neurons (Ramon y Cajal 1911). This premise was strengthened with the discovery of long-term potentiation (LTP) in the HPC, a form of synaptic plasticity whereby a long lasting enhancement of the synaptic response occurs between two neurons following a stimulation event involving coupled activity between the two. Thus, LTP involves a process by which the activity in pre-synaptic fibres leads to an increase in post-synaptic excitation (Eichenbaum 2002). LTP, along with its antithesis long-term depression (LTD), are believed to constitute the mechanism by which behavioural plasticity (i.e. learning and memory) is expressed in the brain. Recent research has shown that changes in the brain similar to those seen during LTP accompany behavioral learning and memory (Rioult-Pedotti et al. 2000; Monfils and Teskey 2004; Whitlock et al. 2006). Based on these findings, it is interesting to note that the network state of the HPC has been found to exert a considerable influence on 1) synaptic transmission and 2) the expression of LTP and LTD.

During the initial phases of study on LTP, the phenomenon was elicited through the application of a tetanus stimulation which was comprised of a relatively long train of constant high frequency (100 Hz) stimulation (Eichenbaum 2002). The problem with this protocol was that it was essentially "hammering" the system with a stimulus that was not

representative of processes that could occur naturally in the brain. Later it was discovered that shorter bursts of stimulation timed to the frequency of the theta rhythm resulted in a LTP effect above that observed from tetanus stimulation (Larson and Lynch 1986; Perez et al. 1999; Hernandez et al. 2005). Further investigation revealed that stimulation timed precisely to the peaks of the ongoing theta rhythm resulted in LTP while stimulation timed to the troughs produced LTD (Hyman et al. 2003). *In vitro* experiments using hippocampal slices have shown that a theta pulse stimulation paradigm (one pulse as opposed to a small burst timed to the frequency of theta) of 30 seconds is sufficient to induce a reliable LTP effect (Thomas et al. 1996; Watabe et al. 2000). In addition, it has been shown in both CA1 (Wyble et al. 2000) and the DG (Buzsáki et al. 1981) that the synaptic response was systematically varied depending on whether the animal was in theta versus LIA. The Wyble paper also went on to describe variation in the synaptic response as a function of the phase of the theta rhythm. The conclusion from this collection of results is that the activity state of the HPC has a significant impact on synaptic responses not only in terms of the presence of different states but as a function of the dynamics within the states themselves. Therefore the alternation between states and the resulting effects on synaptic activity are important factors for the processing of information in the HPC.

Summary

Based on behavioral deficits observed in humans and animals, the HPC has become closely tied to the performance of declarative memory tasks. More specifically the HPC appears to receive and integrate information from the neocortex and form that

information into memories before passing it back to the neocortex for permanent storage. Research on the HPC suggests that synaptic activity, heavily dependent on the spontaneous state of the network in place at the time, is the basis for the processing carried out by the structure. Therefore, we wanted to examine whether changes in hippocampal state would modulate the synaptic response within the main input and output regions of the HPC in a predictable manner considering the proposed encoding and consolidating functions of theta and SO respectively.

We originally speculated that synapses in the CA1 region would show greater excitability during SO while synapses in the DG would exhibit a larger response during theta, based on previous findings and the proposed role of each rhythm. To test this idea we used rats under urethane anesthesia to obtain samples of evoked potentials (EPs) collected during spontaneous alterations of theta and SO (and LIA) as well as periods of induced theta and SO produced by cholinergic manipulation. We found that the synapses of area CA1 did in fact display significantly larger responses during SO. However the synapses in the DG exhibited variable responses ultimately linked to the branch of the PP that was stimulated. Stimulation of the MPP resulted in greater excitability during theta, while stimulation of the LPP produced larger responses in SO. As well, modulation of the synaptic response was found to occur within theta and SO themselves as stimulation on the falling phase of each cycle produced larger responses than stimulation of the rising phase. Finally it was found that the controlled induction of theta or SO through application of cholinergic agonists or antagonists, respectively, produced an effect on synaptic response comparable to or beyond that of the spontaneous activity.

Although a portion of this research was replicating in nature there are several novel findings and contributions put forth by our study. This is the first analysis of EPs in the HPC to investigate the influence that SO has on synaptic activity in and of itself as well as in comparison to other states of the HPC. The fact that SO was found to exert an influence on the synaptic response substantially different from that of theta and LIA supports its existence as a distinctive hippocampal state. Secondly, although previous studies have examined fluctuations in synaptic potentials as a function of ongoing activity in either CA1 or the DG, few have actually looked at both regions at the same time. Because conditions between studies can be varied (different behaviors, different anesthesia) comparisons between them can be compromised. Our study allows a direct comparison between the differences exhibited by area CA1 and the DG. Finally, this is this first study we are aware of to find and report variations between the two branches of the PP in terms of state influenced synaptic response patterns. The findings from our study provide additional support to previous findings while extending knowledge of hippocampal synaptic excitability and the potential mechanisms of memory formation and consolidation.

Figure 1-1. Hippocampal Connections. A Diagram showing the primary flow of information to, from and within the hippocampus (HPC). The neocortex sends projections to the superficial layers of the entorhinal cortex (EC). The medial perforant path (MPP) and lateral perforant path (LPP) carry information from the EC to the dentate gyrus (DG) region of the HPC (1 and 2). The mossy fibre pathway then projects to area CA3 (3). CA3 sends information via the Schaeffer Collaterals to area CA1 (4). CA1 sends axons out of the HPC through the subiculum to the deep layers of the EC (5). The EC then sends axons back to the neocortex.

Figure 1-1

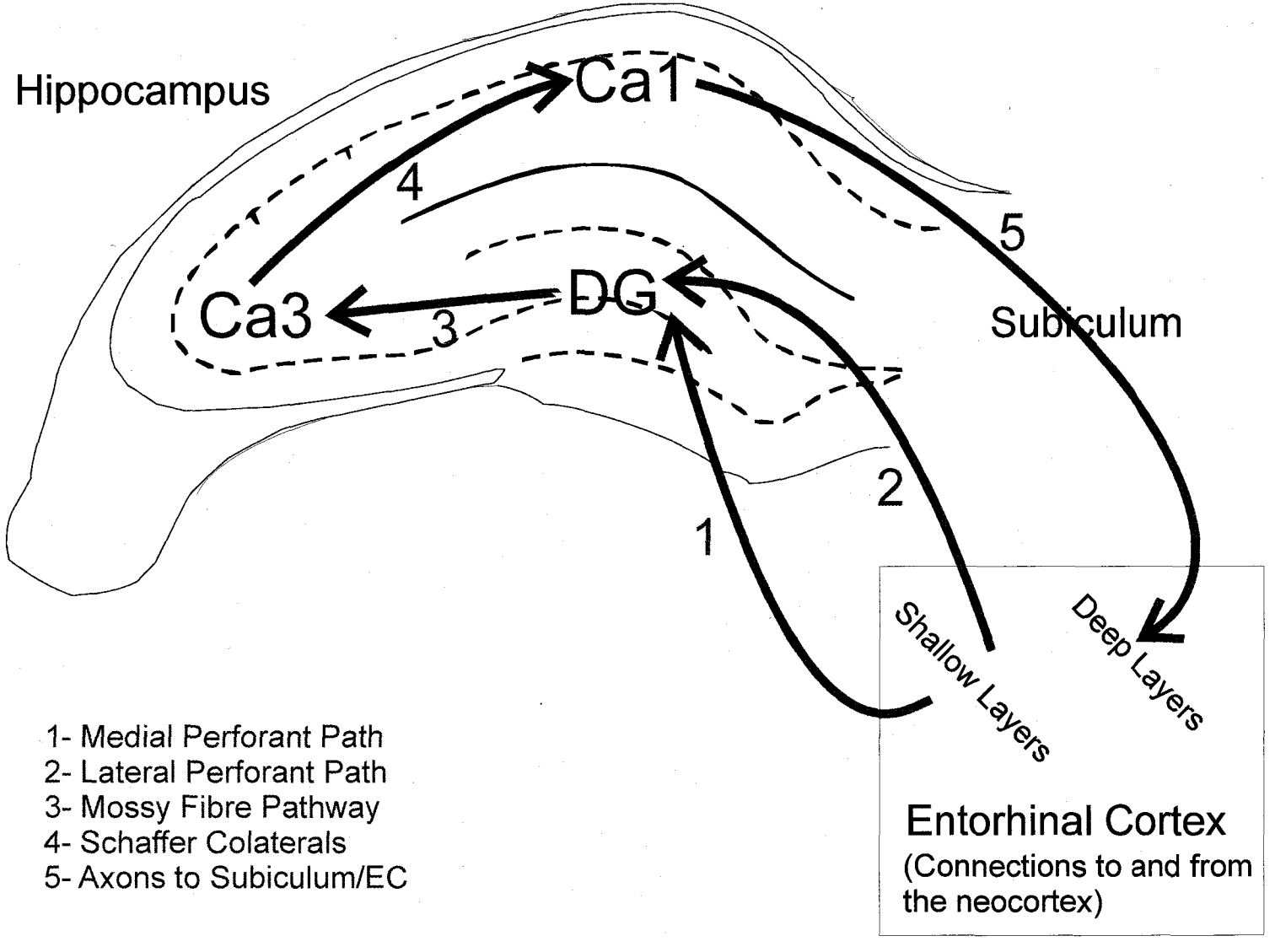

1- Medial Perforant Path
2- Lateral Perforant Path
3- Mossy Fibre Pathway
4- Schaffer Colaterals
5- Axons to Subiculum/EC

References

Alvarez P, Zola-Morgan S, and Squire LR. Damage limited to the hippocampal region produces long-lasting memory impairment in Monkeys. *J Neurosci* 15: 3796-3807, 1995.

Amaral DGL, P. Hippocampal Neuroanatomy. In: *The Hippocampus Book*, edited by Andersen P, Morris, R., Amaral, D., Bliss, T. & O'Keefe, J. New York, New York: Oxford University Press, Inc., 2007.

Andersen JM, Lindberg V, and Myhrer T. Effects of scopolamine and D-cycloserine on non-spatial reference memory in rats. *Behavioural brain research* 129: 211-216, 2002.

Bland BH. The physiology and pharmacology of hippocampal formation theta rhythms. *Prog Neurobiol* 26: 1-54, 1986.

Buzsáki G, Grastyan E, Czopf J, Kellenyi L, and Prohaska O. Changes in neuronal transmission in the rat hippocampus during behavior. *Brain research* 225: 235-247, 1981.

Clark RE, West AN, Zola SM, and Squire LR. Rats with lesions of the hippocampus are impaired on the delayed nonmatching-to-sample task. *Hippocampus* 11: 176-186, 2001.

Corkin S. Lasting consequences of bilateral medial temporal lobectomy - clinical course and experimental findings in HM. *Seminars in Neurology* 4: 249-259, 1984.

Corkin S, Amaral DG, Gonzalez RG, Johnson KA, and Hyman BT. H.M.'s medial temporal lobe lesion: Findings from magnetic resonance imaging. *J Neurosci* 17: 3964-3979, 1997.

Dahl D, and Sarvey JM. Norepinephrine induces pathway-specific long-lasting potentiation and depression in the hippocampal dentate gyrus. *Proc Natl Acad Sci U S A* 86: 4776-4780, 1989.

Eichenbaum H. *The Cognitive Neuroscience of Memory*. New York, New York: Oxford University Press, Inc., 2002.

Eidi M, Zarrindast MR, Eidi A, Oryan S, and Parivar K. Effects of histamine and cholinergic systems on memory retention of passive avoidance learning in rats. *European journal of pharmacology* 465: 91-96, 2003.

Fowler MJ, Sullivan MJ, and Ekstrand BR. Sleep and memory. *Science (New York, NY* 179: 302-304, 1973.

Fredens K, Stengaard-Pedersen K, and Larsson LI. Localization of enkephalin and cholecystokinin immunoreactivities in the perforant path terminal fields of the rat hippocampal formation. *Brain research* 304: 255-263, 1984.

Givens BS, and Olton DS. Cholinergic and GABAergic modulation of medial septal area: effect on working memory. *Behavioral neuroscience* 104: 849-855, 1990.

Haroutunian V, Barnes E, and Davis KL. Cholinergic modulation of memory in rats. *Psychopharmacology* 87: 266-271, 1985.

Hernandez RV, Navarro MM, Rodriguez WA, Martinez JL, Jr., and LeBaron RG. Differences in the magnitude of long-term potentiation produced by theta burst and high frequency stimulation protocols matched in stimulus number. *Brain Res Brain Res Protoc* 15: 6-13, 2005.

Hyman JM, Wyble BP, Goyal V, Rossi CA, and Hasselmo ME. Stimulation in hippocampal region CA1 in behaving rats yields long-term potentiation when delivered to the peak of theta and long-term depression when delivered to the trough. *J Neurosci* 23: 11725-11731, 2003.

Jarrard LE, Feldon J, Rawlins JN, Sinden JD, and Gray JA. The effects of intrahippocampal ibotenate on resistance to extinction after continuous or partial reinforcement. *Experimental brain research Experimentelle Hirnforschung* 61: 519-530, 1986.

Larson J, and Lynch G. Induction of synaptic potentiation in hippocampus by patterned stimulation involves two events. *Science (New York, NY* 232: 985-988, 1986.

Mahut H, Moss M, and Zola-Morgan S. Retention deficits after combined amygdalo-hippocampal and selective hippocampal resections in the monkey. *Neuropsychologia* 19: 201-225, 1981.

McNaughton BL. Evidence for two physiologically distinct perforant pathways to the fascia dentata. *Brain Res* 199: 1-19, 1980.

McNaughton BL, and Barnes CA. Physiological identification and analysis of dentate granule cell responses to stimulation of the medial and lateral perforant pathways in the rat. *The Journal of comparative neurology* 175: 439-454, 1977.

Monfils MH, and Teskey GC. Skilled-learning-induced potentiation in rat sensorimotor cortex: a transient form of behavioural long-term potentiation. *Neuroscience* 125: 329-336, 2004.

Morris RG, Black, A. H. & O'keefe, J. Hippocampal EEG during ballistic movement. *Neuroscience Letters* 3: 1976.

Morris RGM, Garrud P, Rawlins JNP, and O'Keefe J. Place navigation impaired in rats with hippocampal lesions. *Nature* 297: 681-683, 1982.

Pang K, Williams MJ, and Olton DS. Activation of the medial septal area attenuates LTP of the lateral perforant path and enhances heterosynaptic LTD of the medial perforant path in aged rats. *Brain research* 632: 150-160, 1993.

Perez Y, Chapman CA, Woodhall G, Robitaille R, and Lacaille JC. Differential induction of long-lasting potentiation of inhibitory postsynaptic potentials by theta patterned stimulation versus 100-Hz tetanization in hippocampal pyramidal cells in vitro. *Neuroscience* 90: 747-757, 1999.

Plihal W, and Born J. Effects of early and late nocturnal sleep on declarative and procedural memory. *J Cogn Neurosci* 9: 534–547., 1997.

Ramon y Cajal S. Histologie du système nerveux de l'homme et des vertébrés. *trans by L Azoulay Paris: Maloine* 2 vols.: 1911.

Rasch B, Buchel C, Gais S, and Born J. Odor cues during slow-wave sleep prompt declarative memory consolidation. *Science (New York, NY* 315: 1426-1429, 2007.

Rioult-Pedotti MS, Friedman D, and Donoghue JP. Learning-induced LTP in neocortex. *Science (New York, NY* 290: 533-536, 2000.

Rolls ET. Hippocampo-cortical and cortico-cortical backprojections. *Hippocampus* 10: 380-388, 2000.

Scoville WB, and Milner B. Loss of recent memory after bilateral hippocampal lesions. *J Neurol Neurosurg Psychiat* 20: 11-21, 1957.

Squire LR. Memory and the hippocampus: a synthesis from findings with rats, monkeys, and humans. *Psychol Rev* 99: 195-231, 1992.

Stefanacci L, Buffalo EA, Schmolck H, and Squire LR. Profound amnesia after damage to the medial temporal lobe: A neuroanatomical and neuropsychological profile of patient E. P. *J Neurosci* 20: 7024-7036, 2000.

Takashima A, Petersson KM, Rutters F, Tendolkar I, Jensen O, Zwarts MJ, McNaughton BL, and Fernandez G. Declarative memory consolidation in humans: a prospective functional magnetic resonance imaging study. *Proceedings of the National Academy of Sciences of the United States of America* 103: 756-761, 2006.

Thomas MJ, Moody TD, Makhinson M, and O'Dell TJ. Activity-dependent beta-adrenergic modulation of low frequency stimulation induced LTP in the hippocampal CA1 region. *Neuron* 17: 475-482, 1996.

Vanderwolf CH. Hippocampal electrical activity and voluntary movement in the rat. *Electroencephalogr Clin Neurophysiol* 26: 407-418, 1969.

Watabe AM, Zaki PA, and O'Dell TJ. Coactivation of beta-adrenergic and cholinergic receptors enhances the induction of long-term potentiation and synergistically activates mitogen-activated protein kinase in the hippocampal CA1 region. *J Neurosci* 20: 5924-5931, 2000.

Whitlock JR, Heynen AJ, Shuler MG, and Bear MF. Learning induces long-term potentiation in the hippocampus. *Science (New York, NY* 313: 1093-1097, 2006.

Winocur G, McDonald RM, and Moscovitch M. Anterograde and retrograde amnesia in rats with large hippocampal lesions. *Hippocampus* 11: 18-26, 2001.

Witter MP, Naber PA, van Haeften T, Machielsen WC, Rombouts SA, Barkhof F, Scheltens P, and Lopes da Silva FH. Cortico-hippocampal communication by way of parallel parahippocampal-subicular pathways. *Hippocampus* 10: 398-410, 2000.

Wolansky T, Clement EA, Peters SR, Palczak MA, and Dickson CT. The hippocampal slow oscillation: A novel EEG state and its coordination with ongoing neocortical activity. *J Neurosci* 26: 6213-6229, 2006.

Wyble BP, Linster C, and Hasselmo ME. Size of CA1-evoked synaptic potentials is related to theta rhythm phase in rat hippocampus. *J Neurophysiol* 83: 2138-2144, 2000.

Zola-Morgan S, Squire LR, and Amaral DG. Human amnesia and the medial temporal region: enduring memory impairment following a bilateral lesion limited to field CA1 of the hippocampus. *J Neurosci* 6: 2950-2967, 1986.

Zola SM, Squire LR, Teng E, Stefanacci L, Buffalo EA, and Clark RE. Impaired recognition memory in monkeys after damage limited to the hippocampal region. *J Neurosci* 20: 451-463, 2000.

Chapter 2: State Alternations

Introduction

Neural processing in the hippocampus (HPC) is crucial for declarative memory processes (Eichenbaum 2004). One of the major features of the activity in this region is the prevalence of collective oscillatory patterns that are expressed differentially during diverse behaviours and across the various stages of sleep. These synchronized patterns are thought to constrain and modulate hippocampal processing and are also considered as important influences for the expression of synaptic plasticity (Axmacher et al. 2006; Buzsáki 2002; Jensen and Lisman 2005). The two most studied oscillatory patterns in the HPC are the theta rhythm, which is a large amplitude 3-12Hz oscillation that appears during exploratory behaviour and during REM sleep (Bland 1986; Buzsáki 2002; Vanderwolf 1969; Vanderwolf et al. 1977), and sharp wave/ripple complexes, which are transient and irregularly occurring high frequency (150-250 Hz) oscillations that appear during awake immobility, "involuntary" behaviours, and non-REM sleep (Buzsáki 1986; Suzuki and Smith 1987). Due to their different behavioural state-dependencies these two patterns are mutually exclusive and are thought to contribute differentially to sequential stages of memory processing (Buzsáki 1989). Interestingly, both patterns can also be spontaneously and alternately exhibited during urethane anaesthesia (Ylinen et al. 1995a) which provides a tractable system to explore their influence on neurophysiological processing.

Recently, we have described a novel form of collective hippocampal activity – the slow oscillation (SO) (Wolansky et al. 2006). The SO consists of a large amplitude slow (~1Hz) extra cellular rhythm which appears during deep slow-wave sleep as well as

under urethane anaesthesia. This pattern is similar to the slow oscillation that has been described in the neocortex (Steriade et al. 1993) and has been similarly demonstrated to correspond to swings of the membrane potential of hippocampal neurons from depolarized (spiking) levels to hyperpolarized (non-spiking) levels (so-called "up" and "down" states, respectively) (Hahn et al. 2007, 2006; Ji and Wilson 2007; Wolansky et al. 2006) cf. (Isomura et al. 2006). The SO is a state with electrographic and single-unit activity characteristics that separate it from either theta or the large-amplitude irregular activity state (LIA: during which sharp-wave/ripple complexes occur).

Interestingly, the hippocampal SO shows a dynamic and transient correlation with the neocortical SO which would allow for the synchronization (or alternatively desynchronization) of hippocampal and neocortical neuronal ensembles (Wolansky et al. 2006). Thus, the SO could be a candidate platform for establishing bidirectional synaptic plasticity either via long term potentiation or depression in an extended cortico-hippocampo-cortical circuit. Importantly in this regard, recent studies have suggested that non-REM sleep (and in particular the SO) is important for the consolidation of declarative (i.e., hippocampal-dependent) forms of memory (Bodizs et al. 2002; Marshall et al. 2006; Rasch et al. 2007). Given that the SO only appears during non-REM sleep it may be that its pattern of collective brain-wide engagement is central to a systems-level consolidatory process.

In order to examine the influence of this novel state upon the neurophysiological properties of the HPC we performed evoked potential analysis of the connections between areas CA3 and CA1 of the HPC (via the commissural or Schaeffer collateral pathway); between layer II cells of the entorhinal cortex and the dentate gyrus (DG) of

the HPC (the medial perforant path (MPP) and lateral perforant path (LPP)) and between layer III cells of the entorhinal cortex and area CA1 of the HPC (the temporal ammonic (TA) pathway). Our results demonstrate that these pathways can exhibit differential modulation dependent upon state (i.e. greater excitability during either theta or SO) but that all show a rhythmical modulation of excitability that is dependent upon the ongoing phase of the given rhythm.

Materials and Methods

Data were obtained from 29 male Sprague Dawley rats weighing 166 to 370 g (average ± SEM, 262.63 ± 15.06 g. All methods used conformed to the guidelines established by the Canadian Council on Animal Care and the Society for Neuroscience and were approved by the Biosciences Animal Policy and Welfare Committee of the University of Alberta.

Surgical, implantation, recording and stimulating procedures

Animals were initially induced with gaseous isoflurane mixed with medical O_2 at a minimum alveolar concentration (MAC) of 4 in an enclosed anesthetic chamber. After loss of righting reflexes, they were maintained on isoflurane (2.0-2.5 MAC) via a nose cone and implanted with a jugular catheter. Isoflurane was discontinued, and general anaesthesia was achieved using slow intravenous administration of urethane (0.8 g/ml; final dosage, 1.8 ± 0.03 g/kg) via the jugular vein. Body temperature was maintained at 37°C using a servo-driven system connected to a heating pad and rectal probe (TR-100; Fine Science Tools, Vancouver, BC, Canada) for the remainder of the surgical and recording procedures. Level of anaesthesia was assessed throughout the experiment by

monitoring reflex withdrawal to a hind paw pinch. If any visible withdrawal occurred, the animal was administered a supplemental dose (0.01 ml) of urethane.

When the rats no longer exhibited a withdrawal reflex they were moved to a stereotaxic apparatus for electrode placement. Stereotaxic coordinates were calculated from bregma and respective holes were drilled in the skull to allow electrode penetration in the brain. For single electrode recordings, a single microwire (Teflon-coated stainless steel wire with a bare diameter of 125 *u*m; A-M Systems, Carlsborg, WA) was implanted at the level of stratum radiatum of area CA1 (AP, -3.3; ML, $\pm$1.8 to $\pm$2.1; DV, -2.5 to –3.2) or the molecular layer of the DG) (AP, -3.3; ML, $\pm$1.8 to $\pm$2.1; DV, -2.7 to 3.5). These placements were optimised for commissural and perforant path (PP) stimulation, respectively (see further below). In some cases, a 16 contact linear multiprobe (100μm spacing: Neuronexus Technologies, Ann Arbour, MI), was implanted in the vertical plane using the same coordinates as described above for single electrodes. The depth was optimised for recording responses to either or both CA3 or PP stimulation.

For recordings from CA1, evoked potentials (EP) were elicited by stimulating the contra lateral CA3 area using an implanted bipolar electrode constructed from two twisted teflon-insulated stainless steel wires (110 μm bare diameter) at the following coordinates (AP, -3.5; ML, -3.5; DV, -3.0 to -4.0). DG responses were recorded by stimulation of the ipsilateral PP (AP, -7.0; ML, -4.0 to -5.5; DV, -1.5 to –2.5) using an identical electrode. After the recording electrode was lowered into the general area (either CA1 or DG), the stimulating electrode was lowered until a negative-going EP was elicited by stimulating with a 0.2 millisecond biphasic current pulse at an intensity range of 30 to 210 μA) using an isolated constant current pulse generator (model 2100; A-M

Systems, Carlsborg, WA). Both electrodes were then adjusted to ensure a maximal response.

Single electrode (monopolar) recordings were referenced to ground (stereotaxic apparatus) and amplified at a gain of 1000 and filtered between 0.1 and 500 Hz using a differential AC amplifier (model 1700; A-M Systems). Signals from the probe were also referenced to ground and amplified at a final gain of 1000 and wide-band filtered between 0.7Hz and 10 kHz via a 16-channel head stage (unity gain) and amplifier system (Plexon, Dallas, TX). All signals were digitized with a Digidata 1322A A-D board connected to a Pentium PC running the AxoScope acquisition program (Molecular Devices; Union City, CA). Signals were sampled at 1 kHz or above and were digitized online after being low-pass filtered at 500Hz (software controlled).

Experimental Procedure

After suitable sites were located, an input/output curve was constructed by recording the response evoked at increasing levels of intensity of stimulation. In this way both threshold and maximal values of current injection could be assessed. Subsequently, EPs were elicited at a stimulus intensity which evoked a population excitatory post-synaptic potential (pEPSP, also referred to as a field EPSP) at 70% of the maximum response. It was ensured that for experiments involving slope measurements of the pEPSP component of the EP that the current intensity used did not produce a population spike. The interstimulus interval was 8s or greater. In all experiments an average EP or EP profile was recorded using a minimum of 16 sweeps. In experiments where the effects of stimulation of the PP were assessed using the multiprobe an average paired pulse profile (using an inter-pulse interval of 50ms) was also recorded. Continuous

recordings of spontaneous EEG (i.e. hippocampal local field potential) activity were also made over a 10-20 minute period and ensured that alternations between activated (theta) and deactivated (SO) states were spontaneously occurring in the HPC (Wolansky et al. 2006). Following recording of these spontaneous records, EPs were collected every 10s across both spontaneous theta and slow oscillation states. Sweeps were 8s in length, which was long enough to allow a positive determination of state based on spectral and autocorrelation analysis of sweeps. In addition, it allowed for a determination of the phase of the spontaneous cycle at the point of stimulation (2-3 seconds into the sweep).

After recording sessions, a small lesion was made at the tip of all single recording and stimulating electrodes by passing 1 mA of DC current for 5 seconds using an isolated constant current pulse generator (model 2100; A-M Systems). To make the multiprobe track visible for histological purposes, the probe was moved slightly in two horizontal planes at its most ventral position.

Histological Procedure

Rats were perfused transcardially, initially with physiological saline then with 4% Para formaldehyde in saline. Brains were extracted and stored overnight in 30% sucrose in 4% Para formaldehyde. The tissue was frozen with compressed CO_2 and sliced at 60 μm with a rotary microtome (1320 Microtome; Leica, Vienna, Austria). Slices were then mounted on gel-coated slides, allowed to dry for a minimum of 24 h, subsequently stained using thionin and cover slipped. Microscopic inspection of stained slices was used to verify recording loci. Digital photomicrographs (Canon Powershot S45; Canon, Tokyo, Japan) were taken on a Leica DM LB2 microscope, imported using Canon

Remote Capture 2.7 software and processed with Corel PhotoPaint (Corel, Ottawa, Ontario, Canada).

Data Analysis

Population EPSP slope and state measurements

The slope of the population pEPSP response was assessed by fitting a line to the initial negative component of the EP (Clampfit version 9.0 Molecular Devices, Union City, CA). Slopes were computed for individual trace and were then averaged and compared as a function of EEG state and the phase of the ongoing spontaneous oscillation cycle. Slope measurements of the pEPSP component were chosen over measures of amplitude since the former correlate directly with the strength of synaptic transmission and are less subject to spurious field artefacts (Johnston and Wu 1995, pp 432-435). EEG state was classified as theta or SO based on the power spectrum and autocorrelation computed for each trace (Wolansky et al. 2006). Threshold power values for each of the SO (0.5 to 1.5 Hz) and theta (3 to 4 Hz) bandwidths were computed from the temporal variation of power values within these bandwidths derived from spontaneous EEG collected prior to stimulation trials. Traces that had supra-threshold power values for the SO and sub-threshold power values for theta bandwidths were designated as SO while conversely traces with supra-threshold power values for theta and sub threshold power values for SO bandwidths were designated as theta. Confirmation of a rhythmic state was achieved by subsequent assessment of rhythmicity in the autocorrelation function (Wolansky et al. 2006). Traces without rhythmicity were classified as LIA.

Oscillatory phase determination

For confirmed rhythmic states (either theta or the SO), the phase value at which the EP was triggered was calculated by fitting a sine wave to the bandwidth filtered EEG (3 to 4 Hz for theta and 0.5 to 1.5 Hz for SO). Phase was computed relative to the upward zero crossings of the oscillatory signal directly before and after the EP as a function of the period of the full sine wave connecting these two zero crossings. These values were then translated to a degree scale (from 0 to 360) where 0 signified the initial upward zero crossing, 90 the positive peak, 180 the downward zero crossing, 270 the negative peak and 360 the final upward zero crossing of the sine function. Slope values of the pEPSP were measured as above for individual EPs. In order to eliminate any contamination of the ongoing rhythm to these slope measurements, we also computed slope values of the field activity just prior (50 ms) to the stimulation and subtracted these values from the pEPSP slope measurements (Wyble et al. 2000). Averaged slope values across phase windows were normalized to both their minimum and maximal values within each experiment in order to compute summary statistics.

Current source density

Current source density (CSD) analysis was conducted on spontaneous and averaged field potential profiles recorded using the linear multiprobe following the assumptions of (Freeman 1975; Ketchum and Haberly 1993; Rodriguez and Haberly 1989). An advantage of this form of analysis is that it is completely immune to volume-conducted potentials since it provides an estimate of transmembrane current flow (Johnston and Wu 1995, pp 435-438). Briefly, CSD was computed by estimating the second spatial derivative of unfiltered voltage traces derived from the multiprobe. This

estimate was calculated using a three-point difference (differentiation grid size of 300 μm) on the voltage values across spatially adjacent traces:

$$CSD = [f(p_{i-1})-2f(p_i)+f(p_{i+1})]/d^2 \quad \text{(Equation 1)}$$

Where $f(p_i)$ is the field signal from probe channel i ($i = 2, 3, \ldots, 14$) and d is the distance between adjacent channels (0.1mm).

Data summary and statistics

Arithmetic averages were computed within and between experiments and were reported together with the standard error of the mean (SEM). Comparisons of interest were conducted using one-tailed paired t-tests using an alpha (probability) value of 0.05. Descriptive circular statistics using the method of Batschelet (as described by (Zar 1999) pp 608-610) were used to compute the oscillatory phase angle at which pEPSPs were preferentially maximal on binned slope data (bin width: 18°). Normalized slope values were used as vector lengths for each of the centre points of the phase angle windows. These analyses were conducted on both individual experiments and the average across all experiments. The distribution of the preferred phases across all individual experiments was tested for homogeneity using the method of Hotelling (as described by (Zar 1999) pp 638-639).

Results

Histological findings

We confirmed the location of all single electrode and multiprobe locations. All CA1 recording positions were in the mid-apical dendritic layer of CA1 pyramidal cells (centered at stratum radiatum or at the border with stratum lacunosum moleculare). All

DG recording positions were at the level of the hippocampal fissure or lower (in the molecular layer of the DG). Stimulation sites in the contra lateral CA region were in or near CA3. These sites could be close to the lower blade of the CA3 pyramidal layer, in the mid-apical dendritic zone of stratum radiatum of CA3 at the level of its vertical curvature or in stratum radiatum close to the CA1/CA3 border. Stimulation sites aimed at the PP were found to be in or just superior to the dorsal element of the angular bundle. Multiprobe tracts were all in a plane that traversed the CA1 pyramidal cell layer, through the hippocampal fissure and the DG. The termination of probe tracts was typically in stratum granulosum or in the hilar region of the DG just ventral to the granule cell layer. The position of individual contact sites was estimated from the position of the histological tract in combination with comparisons to the distribution of spontaneous (theta and SO) and evoked potential profile measures (Wolansky et al. 2006). Summary placements and tracks for all experiments are shown in Figure 1.

State alternations

As previously described (Wolansky et al. 2006) the activity of the HPC spontaneously alternated between activated (theta), transition (large amplitude irregular activity: LIA), and deactivated (SO) patterns. All EPs were elicited during and across these spontaneous patterns. By performing spectrographic and autocorrelation analysis of ongoing EEG (Wolansky et al. 2006) for each stimulation trial, we were able to differentiate between all three states. Typical examples of hippocampal theta and slow-oscillatory states are shown in Figure 2. As demonstrated, theta was characterized by highly rhythmic oscillations in the frequency bandwidth of 3 to 5 Hz while the SO was characterized by even larger amplitude rhythmic oscillations in the 0.5 to 1.0 Hz frequency bandwidth. In

comparison, LIA showed a lack of rhythmicity with high power levels across a wider range of the spectrum without clear frequency peaks.

Influence of State on Evoked Potentials

CA3-CA1 EPs

EPs elicited by stimulation of contra-lateral CA3 and recorded at the level of stratum radiatum in CA1 were similar to pEPSPs as previously described (Wyble et al. 2000). They exhibited a maximum negative peak at a latency of 13.07 ± 1.61 ms post-stimulation. A typical evoked potential is shown in Figure 3. Spontaneous alternations between theta, LIA and SO states resulted in significant variations of synaptic excitability as measured by changes in the slope of the pEPSP. Slope values were consistently (5 out of 5) and significantly ($t= 5.66$, $p=0.0024$) larger during periods of SO as compared to periods of theta. Slope values measured during LIA were intermediate but significantly different to those measured during theta ($t= 4.63$, $p=0.0049$) and the SO ($t= 5.19$, $p=0.0033$) (Figure 4).

Multiprobe recordings through the CA1 region and centred at the level of stratum radiatum were conducted in order to further explore the voltage and current source density (CSD) profiles of CA3 stimulation-evoked EPs. As previously described, the most prominent sink was observed at the level of stratum radiatum, which also corresponded to the time point of maximal negativity of the evoked potential in this region (12.09 ± 0.49ms – see Figure 5). More importantly, however, the magnitude of this sink was consistently larger during the SO than during theta in this, and all other experiments, and was significantly larger during the SO overall (SO: 102.61 ± 32.23; TH: 88.01 ± 26.65; $t(4) = 3.96$, $p=0.008$: $n= 5$) (Figure 5).

Perforant path – Dentate gyrus EPs

EPs elicited by stimulation of the PP and recorded at the level of stratum moleculare in the DG exhibited a maximum negative peak occurring 3-8 ms post-stimulation. This EP was consistent with pEPSP responses previously described in this region (Canning and Leung 1997; Canning et al. 2000; Leung et al. 1995). Assessment of the variation of synaptic excitability across states through measurement of pEPSP slopes produced mixed results. Comparing theta to SO, three out of five experiments had significantly larger slope values in SO while the other two had significantly larger slope values during theta. In all cases, slope values during LIA were intermediate to those found during theta and SO. In the three experiments in which slopes were largest during the SO, those evoked during LIA were significantly different from both SO and theta in one, and significantly different from SO (but not theta) in the remaining two (Figure 6). In the two experiments in which slopes were largest in theta, those evoked during LIA were significantly different from theta (but not SO) in one and from SO (but not theta) in the other.

During these initial experiments we did not differentiate between the various components of the PP (MPP vs. LPP vs. TA). In order to determine if these different input pathways from the EC to the HPC demonstrated different levels of modulation according to state we attempted to separate them by mapping their different spatio-temporal properties using simultaneous profile recordings and by assessing their responsiveness to paired pulse stimulation at short latencies. Since the medial, lateral and temporal ammonic branches of the PP have different laminar terminations zones (MPP: middle third of the DG molecular layer; LPP: outer third of the DG molecular layer; TA:

stratum lacunosum molecular of CA1) and the shape and latency of activation of each of these components are slightly different (MPP < LPP < TA) (Abraham and McNaughton 1984; Canning and Leung 1997; Canning et al. 2000; Leung et al. 1995; McNaughton 1980), the EPs evoked by each of these pathways could be separated. As well, at paired pulse intervals of 50ms, the MPP demonstrates depression while the LPP and the TA pathway demonstrate facilitation (Leung et al. 1995; McNaughton 1980). In this way, we were able to determine the identity of the primary pathway (if any) that was activated.

Using these criteria we were able to separate MPP, LPP and TA components of the EPs, even in single experiments as shown in Figures 7 and 8 In accordance with previous findings (Abraham and McNaughton 1984; Canning and Leung 1997; Canning et al. 2000; Leung et al. 1995; McNaughton 1980), MPP pEPSPs had shorter peak latencies (4.12 ± 0.20 ms) than LPP pEPSPs (5.48 ± 0.14 ms) while pEPSPs generated by TA stimulation showed the longest peak latencies (6.50 ± 0.21 ms). As well, at 50ms intervals, paired pulse potentials evoked by MPP stimulation showed depression (on average: 12.5 ± 3.1 percent) while both LPP and TA EPs were facilitated (on average: 11.4 ± 1.4 percent and 17.2 ± 2.1 percent, respectively).

More importantly, pEPSPs evoked by stimulation of the MPP as opposed to the LPP and the TA showed opposing relationships with respect to state. The pEPSP slopes of MPP EPs were smaller during SO as compared to theta in four of five experiments and showed a trend to be smaller overall. In general, values during LIA were intermediate, and while they were only significantly different from values during theta in one experiment they were significantly larger than values during SO in three of the five experiments (Figure 7A).

In contrast, the slopes of LPP pEPSPs were consistently larger during SO as compared to theta in all (n=5) experiments and were significantly greater overall ($t(4) = 3.15$, $p=0.017$) (Figure 7). On average, slope values during LIA were not significantly different to those during theta overall although in most experiments (four out of five) they were intermediate between theta and SO values (Figure 7). However, values during LIA were significantly lower overall as compared to those measured during SO ($t(4) = 2.28$, $p= 0.0042$).

Similarly to results for the LPP, the slope of TA pEPSPs were consistently larger during SO as compared to theta in all (n=6) experiments (Figure 7) and were significantly greater overall ($t(5) = 3.03$, $p=0.014$). On average, slope values during LIA were intermediate between theta and SO (Figure 7)and while they were significantly different from those during SO ($t(5) = 3.08$, $p= 0.0014$) they were not significantly different from those during theta.

Further support of this differentiation was obtained in experiments where we conducted multiprobe recordings through CA1 and the DG (Figure 8). These experiments allowed us to explore the voltage and CSD profiles of PP stimulation-evoked EPs. In some cases (and as shown in Figure 8), we were able to distinguish all pathways simultaneously. As previously described (Canning et al. 2000), different sinks could be separated based on their spatio-temporal profile corresponding to MPP, LPP, and TA (see above and Figure 8). Confirmation of different pathways was provided by conducting paired pulse stimulation and with a combination of histological and profile analysis of spontaneous rhythms (Wolansky et al. 2006). The average magnitude of sinks at these different levels across states were consistent with the slope results for each pathway. For

the MPP, sinks were consistently (5 out of 5 experiments) and significantly ($t(4) = 2.54$, $p= 0.032$) lower in amplitude during the SO as compared to theta. For the LPP and TA, sinks were consistently (4 out of 5 and 4 out of 4 experiments, respectively) and significantly larger in amplitude during the SO as compared to theta (LPP: $t(4) = 2.28$, $p= 0.043$; TA: $t(3) = 3.95$, $p= 0.014$) (Figure 8).

Influence of Oscillatory Phase on Evoked Potentials

In many of our experiments we noted that there was substantial variation of slope values within each of the oscillatory field states of theta and SO. Previous studies have shown that synaptic excitability as measured by the slope of the pEPSP is related to the phase of the ongoing theta rhythm and is an important factor in the development of LTP (Greenstein et al. 1988; Hyman et al. 2003; Pavlides et al. 1988; Wyble et al. 2000). We were interested in determining whether the phase of the ongoing SO rhythm in the HPC could also modulate excitability in a similar way. Therefore, we tested the influence of phase of both rhythms on the slope of evoked pEPSPs at all sites. A typical experimental protocol is shown in Figure 9 using CA1 responses to CA3 stimulation during theta as an example.

In support of previous findings exhibiting phase influences on synaptic activity during theta (Holscher et al. 1997; Hyman et al. 2003; Rudell and Fox 1984; Rudell et al. 1980; Wyble et al. 2000) and as shown in Figure 9, we found that the phase of the theta cycle had an obvious influence on the size and slope of pEPSPs. By separating evoked potentials based on whether they occurred on the rising or falling phases of the theta rhythm we were able to demonstrate a significant difference in the average slope values. As shown for the example in Figure 9, the size and slope of the pEPSP was larger during

the falling phase and the average difference across multiple trials in the same experiment was significant ($t(50)=2.62$, $p=0.009$).

A similar analysis was conducted for both theta and the SO across all experiments. The average results for CA1 and DG EPs are shown in the left-most panels in Figure 10 (***ai*** and ***bi***, respectively). In all cases, there was a significant and similar effect on pEPSP slopes when comparing the rising vs. the falling phases of ongoing oscillatory activity. We found no differences in the DG responsiveness to stimulation of the different branches of the PP and thus these data were pooled. Slope values were always significantly larger during the falling as opposed to the rising phase (CA3-CA1 theta: $t(3) = 4.84$, $p<0.001$; CA3-CA1 SO: $t(4) = 3.17$, $p=0.011$; PP-DG theta: $t(5) = 5.65$, $p<0.001$; PP-DG SO: $t(5) = 5.65$, $p<0.001$).

In order to more carefully characterize this phase-dependent effect, we arranged stimulation trials in twenty equally-sized bins (18° wide) across the entire cycle and assessed the average normalized pEPSP slope as a function of the phase window in which they occurred. The oscillatory phase angle at which pEPSP slope was preferentially maximal was computed for each experiment and these results are plotted in the middle panels of Figure 10 (CA1: ***aii***; DG: ***bii***). As can be seen, the preferred phase angles for both theta (small filled circles) and the SO (small open circles) for every experiment (except one SO example in the DG) was located in a cluster on the left half of the unit circle between 90 and 270 degrees (i.e. on the falling phase of the ongoing field cycle). The distribution of these values was subjected to a second-order analysis (see Methods section) and the average preferred angle across all experiments calculated (TH: large filled circles; SO: large open circles). In every case these averages were distributed close

to 180° (**CA1:** TH 167°, SO 160°; **DG:** TH 166°, SO 191°). With the exception of the SO in the DG, these distributions were all significantly different from homogeneity (**CA1:** TH $f(2,2) = 44.26$, $p<0.05$; SO $f(2,3) = 13.48$, $p<0.05$; **DG:** TH $f(2,4) = 19.18$, $p<0.05$; SO $f(2,4) = 2.92$, $p>0.05$).

An average distribution of normalized slope values across phase bins was also calculated across all experiments and is shown in the right-most panels of Figure 10 (CA1: ***aiii***; DG: ***biii***). For illustrative purposes, a sine wave delineating the field cycle is superimposed on the data for theta (closed squares) and SO (open squares). There is a clear cyclical modulation of slope values as a function of the ongoing phase of the field cycle for both TH and SO in both regions. These distributions were further subjected to a circular statistical analysis. The average preferred angle is denoted for both theta (closed arrowhead) and SO (open arrowhead) for each of the distributions. Again, these values were located on the falling phase of the ongoing field cycle and were similar to those reported above (**CA1:** TH 167°, SO 153°; **DG:** TH 165°, SO 181°).

Discussion

Consistent with past research (Buzsáki et al. 1981; Fox 1989; Leung 1980; Segal 1978; Winson and Abzug 1978; Wyble et al. 2000), we have confirmed that spontaneous fluctuations in hippocampal electrographic state produced a significant modulation of synaptic excitability in a variety of hippocampal pathways. Importantly, three novel findings have emerged: 1) The direction of changes in synaptic excitability across states was specific for the particular pathway studied. Our data complement and extend those of previous researchers who documented opposite changes with state when comparing PP

stimulation with CA3 stimulation (Herreras et al. 1988; Winson and Abzug 1978) by further showing that stimulation of the two branches of the PP (medial and lateral) yielded independent and contrasting state-dependent effects. This demonstrates that electrographic state in the hippocampal network provides an even more complex modulation of inputs arriving to and being processed by the HPC than originally thought. 2) The recently described SO state (Wolansky et al. 2006) promoted changes in hippocampal excitability that distinguish it from both the theta and LIA states. Thus, this provides further evidence that the SO is a separate and specific state of hippocampal activity. 3) Significant variations of excitability within the rhythmic state of SO, (similar to our and others results for theta) were predicted by the ongoing phase of the field cycle. Altogether, these findings have important implications for the processing and storage of information by the HPC and may provide clues to the communication and potential consolidation strategies employed in the cortico-hippocampo-cortical circuit that are crucial for declarative memory processes.

Significance of state-dependent fluctuations in hippocampal excitability

Hippocampal processing is well known to be important for mnemonic processes (Eichenbaum 2004; Squire 1992). Its memory-related functions are thought to be engaged not only during wakefulness, when learning occurs and behavioural performance is engaged, but also during the patterns of activity that occur during "resting" periods (e.g. sleep) subsequent to the learning process (Born et al. 2006; Walker and Stickgold 2004). It is these patterns (such as those differentially expressed during REM and non-REM stages of sleep) which are thought to contribute to the long-term consolidation of declarative memories (Buzsáki 1989; Marshall et al. 2006; Rasch et al. 2007).

Recently we have shown that the expression of state-dependent alternations of activity that are present during sleep can also occur spontaneously under urethane anaesthesia and that the similarities between the two suggest that urethane is a good model system for sleep itself (Clement et al. 2006; Dickson et al. 2007a; Dickson et al. 2007b). Indeed, and more specifically for collective activity in the hippocampus, previous researchers have exploited urethane as a model for a number of different patterns of hippocampal activity that are expressed during sleep including theta, gamma, and sharp-waves (Penttonen et al. 1998; Ylinen et al. 1995a; Ylinen et al. 1995b). Indeed, the theta state has a similar and overlapping bandwidth (3-6Hz in urethane vs. 4-7Hz in REM sleep (Leung 1985; Vanderwolf et al. 1977)) and the SO has an identical bandwidth (centred at 1Hz) across urethane anaesthesia and slow-wave sleep (Wolansky et al. 2006). As well, both states across urethane and sleep are affected in the same fashion by cholinergic agents: Theta is promoted by muscarinic agonism, whereas the SO is promoted by muscarinic antagonism (Robinson et al. 1977; Wolansky et al. 2006).

Our present findings suggest that the spontaneously expressed and state-dependent patterns of activity observed in the HPC differentially regulate excitability in hippocampal input and output pathways. For example, CA1 excitability was observed to be maximal during the SO in response to stimulation of either CA3 or TA. Given that the SO is a prominent component of deep stages of slow-wave sleep, this implies that the output of CA1 is preferentially biased during these stages. Furthermore, given the dynamic correlation of the SO across the HPC and nCTX (Wolansky et al. 2006), this would mean that the timing of hippocampal output could be systematically synchronized and/or desynchronized with that in the nCTX. The coupling and decoupling of

hippocampal and cortical ensembles achieved in this manner would be highly relevant for the associative and activity-dependent processes of long-term potentiation (LTP) and long-term depression (LTD) and could thus constitute a platform for the process of declarative memory consolidation.

Interestingly, and in contrast to the results for CA1, input to the DG was differentially modulated by state depending on which branch of the PP was stimulated. MPP stimulation produced a maximal response during theta while LPP stimulation produced a maximal response during the SO. Responses during LIA, although variable, were intermediate to those between theta and the SO. This variability might be attributable to the difficulty in separating the stimulation and recording sites for each of the branches of the PP since most experiments had overlapping activation of both branches. However, the significant difference between the theta and SO states suggests that input from the medial EC via the MPP is preferentially processed by the DG during REM sleep while input from the LPP via the lateral EC is preferentially processed by the DG during slow-wave sleep. The relevance of this difference is less clear although previous work has demonstrated differences in the hodological (Witter et al. 2000), physiological (Abraham and McNaughton 1984; Alonso and Klink 1993; Dahl et al. 1990; McNaughton 1980; Tahvildari and Alonso 2005), pharmacological (Bramham et al. 1988; Dahl and Sarvey 1989) and behavioural (Ferbinteanu et al. 1999; Hargreaves et al. 2005) significance of these two pathways in addition to the medial and lateral regions of the EC that give rise to them. State-dependent segregation via preferential processing of these two inputs at the level of the DG may very well have implications for the functional separation of episodic versus semantic declarative memory processes (Eichenbaum 2004, 2006).

Although mentioned above, another finding related to the differential excitability of hippocampal input pathways relates to the TA. Like the LPP, the TA showed preferential excitability during the SO suggesting that the direct entorhinal-CA1 pathway from EC is preferentially excitable during slow-wave sleep. One ramification of this would be enhanced reverberatory communication between the HPC and the EC within the entorhino-hippocampal loop (ECIII – CA1 – ECV – ECIII). The functionality of this reverberatory loop has been demonstrated physiologically (Kloosterman et al. 2004) and the importance of the TA in hippocampal-dependent mnemonic function has been demonstrated (Brun et al. 2002; Remondes and Schuman 2004). Oscillatory and synchronized reverberations within this circuit might mediate the solidification of medial temporal lobe representations during slow wave sleep.

Although our study of hippocampal pathways was extensive, further study of state-dependent influences in the remaining elements of the trisynaptic pathway is required. In particular, the mossy fibre pathway (DG-CA3) and the hippocampo-cortical pathway (CA1 to subiculum and EC) may show important differences in regards to state-dependent modulation. Indeed, previous work suggests that the deep layers of the EC may be preferentially responsive to slow patterned activity as opposed to theta (Yun et al. 2002).

State-dependent changes in excitability of hippocampal circuitry are not only important for an understanding of physiological functioning but may also be relevant for pathology – especially that concerning epilepsies deriving from the medial temporal lobe. It is well known that certain forms of epilepsy can be expressed more prevalently during sleep, especially during non-REM stages (Foldvary-Schaefer and Grigg-Damberger

2006) . Our findings might also be relevant for the sleep-related preponderance of epileptiform events deriving from medial temporal lobe structures (Herman et al. 2001). The SO may effectively reduce the threshold for hypersynchronous discharges in the HPC and may also result in an increased ability to generalize through cortical output pathways via the entorhinal cortex and medial temporal lobe (Herman et al. 2001). Further research is necessary to examine this possibility.

Cycle by cycle modulation of hippocampal excitability

Not only was state an important modulator of synaptic responsiveness but within each rhythmic state, whether theta or the SO, so too was the phase of the oscillatory field cycle. Such modulation provides the HPC with an even more fine-grained temporal mechanism to influence processing. In both CA1 and DG regions the slope of the EP was larger during the falling phase of the cycle than the rising phase and excitability was systematically modulated across phases. Although previous researchers have documented similar results for the theta rhythm (Buzsáki et al. 1981; Rudell and Fox 1984; Rudell et al. 1980; Wyble et al. 2000) this is the first demonstration of such a cyclical modulation for the SO in the HPC.

For both cycles, the falling phase of the extra cellular field potential rhythm corresponds to a transition point where the net flow of current is moving out of the extra cellular medium and entering the intracellular space. At the intracellular level, this corresponds very simply to a transition from a more hyperpolarized level to one that is more depolarized. Thus, the timing of enhanced synaptic efficacy is set to the period at which the membranes of postsynaptic neurons are moving towards the just-subthreshold range. Synaptic input arriving at these moments are likely to bring the post-synaptic

membrane to threshold and discharge the cell earlier in the cycle than would occur spontaneously. A similar mechanism which additively couples linearly increasing excitation with subthreshold oscillatory activity is proposed to underlie the phase precession shown by hippocampal place cells relative to the ongoing theta rhythm as the animal passes through its spatial receptive field (Harris et al. 2002; Mehta et al. 2002; O'Keefe and Recce 1993). Our results show that there may also be a further cyclic modulation of synaptic excitability with respect to the field oscillation that is also phase-locked to the ongoing oscillation. One effect that this might have would be to extend the effective phase range of precession that is possible within an oscillatory cycle. Although it is unclear how phase precession occurring through phase-coupled enhancements in synaptic transmission might be important for processing during either hippocampal theta or SO within sleep, certainly the relative timing of discharge with respect to other neurons would have functional implications for ensemble binding and for plasticity (Holscher et al. 1997; Hyman et al. 2003; Pavlides et al. 1988).

Figure 2-1. Summary of Histological Placements. Dots show the placements of recording and stimulating electrodes for (A) CA3-CA1, (B) PP-Dentate gyrus (DG), and (C) multiprobe recordings.

Figure 2-1

A. CA3-CA1

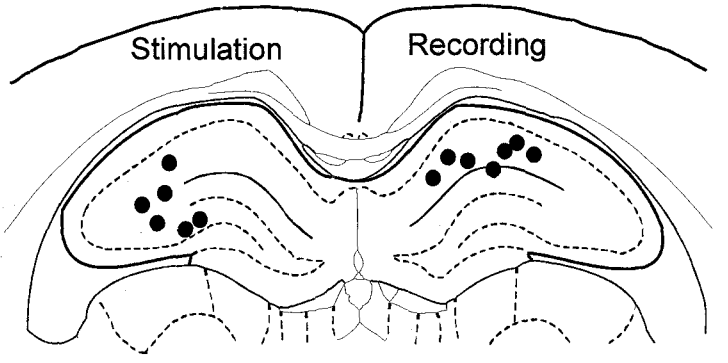

B. PP-DG

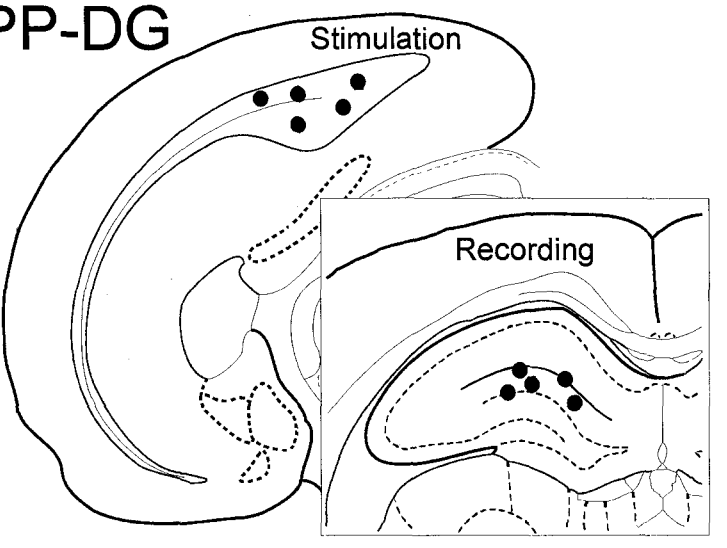

C. Multiprobe

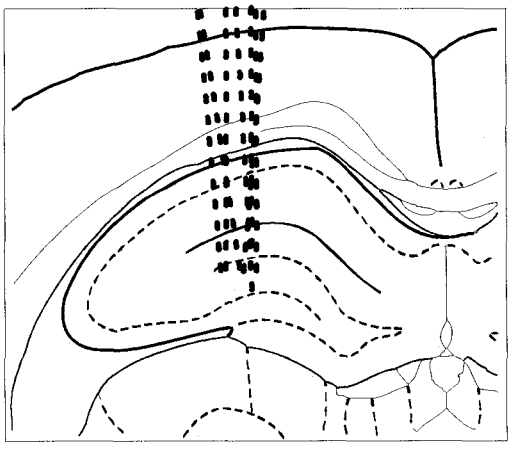

Figure 2-2. State-Dependent Activity under Urethane Anesthesia. Spontaneous hippocampal field activity can be classified into three states: theta, large-amplitude irregular activity (LIA) or the slow oscillation (SO). Raw traces for each of the three states are shown in **A)** with their corresponding power spectra and autocorrelograms (insets) in **B)**. Each state can be differentiated based on the raw signal as well their respective power spectrums and autocorrelations. Theta and the SO are characterized by their rhythmic patterns in the 3-4 Hz and 1 Hz bandwidths, respectively while LIA is characterized by a broad bandwidth non-rhythmic pattern.

Figure 2-2

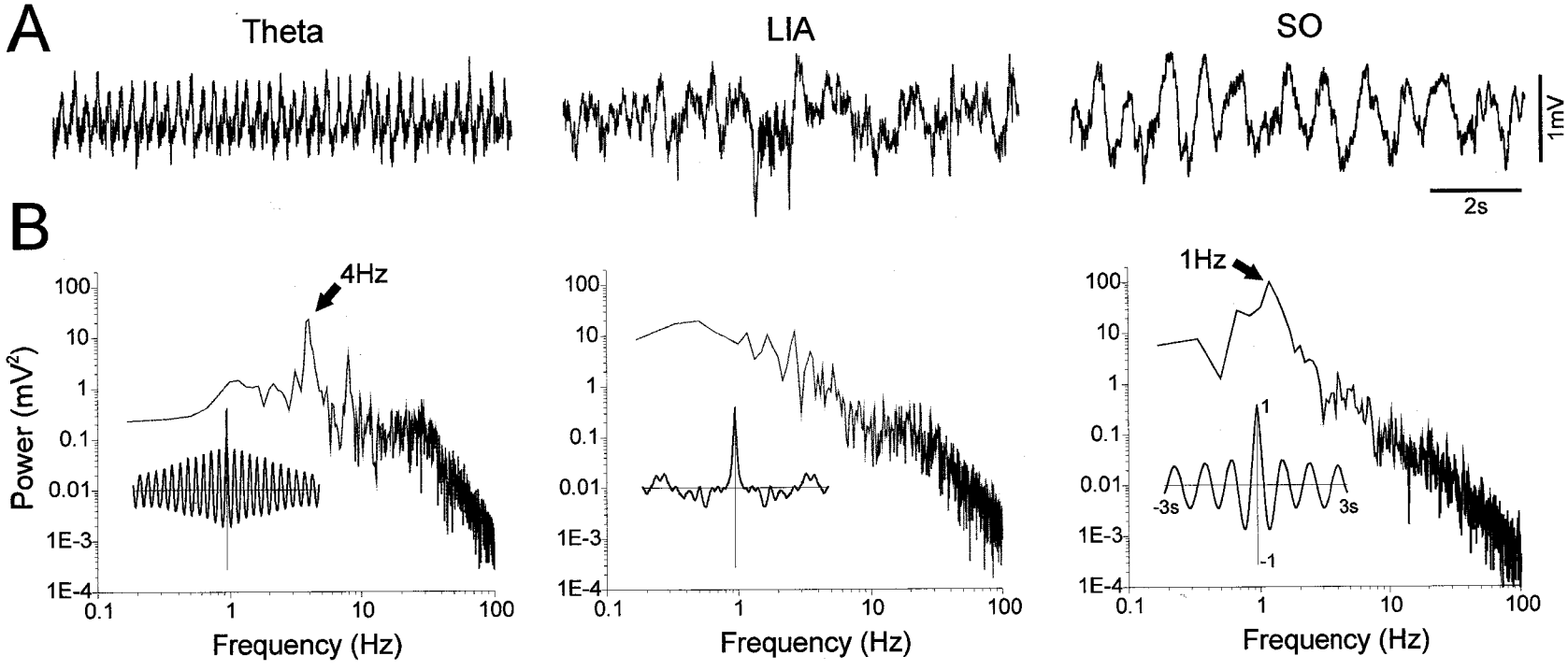
A
Theta
LIA
SO
1mV
2s
B
4Hz
1Hz
Power (mV²)
Frequency (Hz)
100
10
1
0.1
0.01
1E-3
1E-4
0.1
1
10
100
-3s
3s
1
-1

Figure 2-3. Influence of State on Evoked Potentials. **A)** Evoked potentials (EPs: highlighted by grey shading) were elicited during ongoing theta (top) and the slow oscillation (SO: bottom) in CA1 via contralateral CA3 stimulation. **B)** Power spectra of the spontaneous field potentials confirmed the difference between ongoing states and **C)** average expanded and superimposed sweeps of the EPs across the two states demonstrates a larger EP during the SO as compared to theta. **D)** Average values of the pEPSP slopes show a significant difference between states with negative slope values higher during the SO.

Figure 2-3

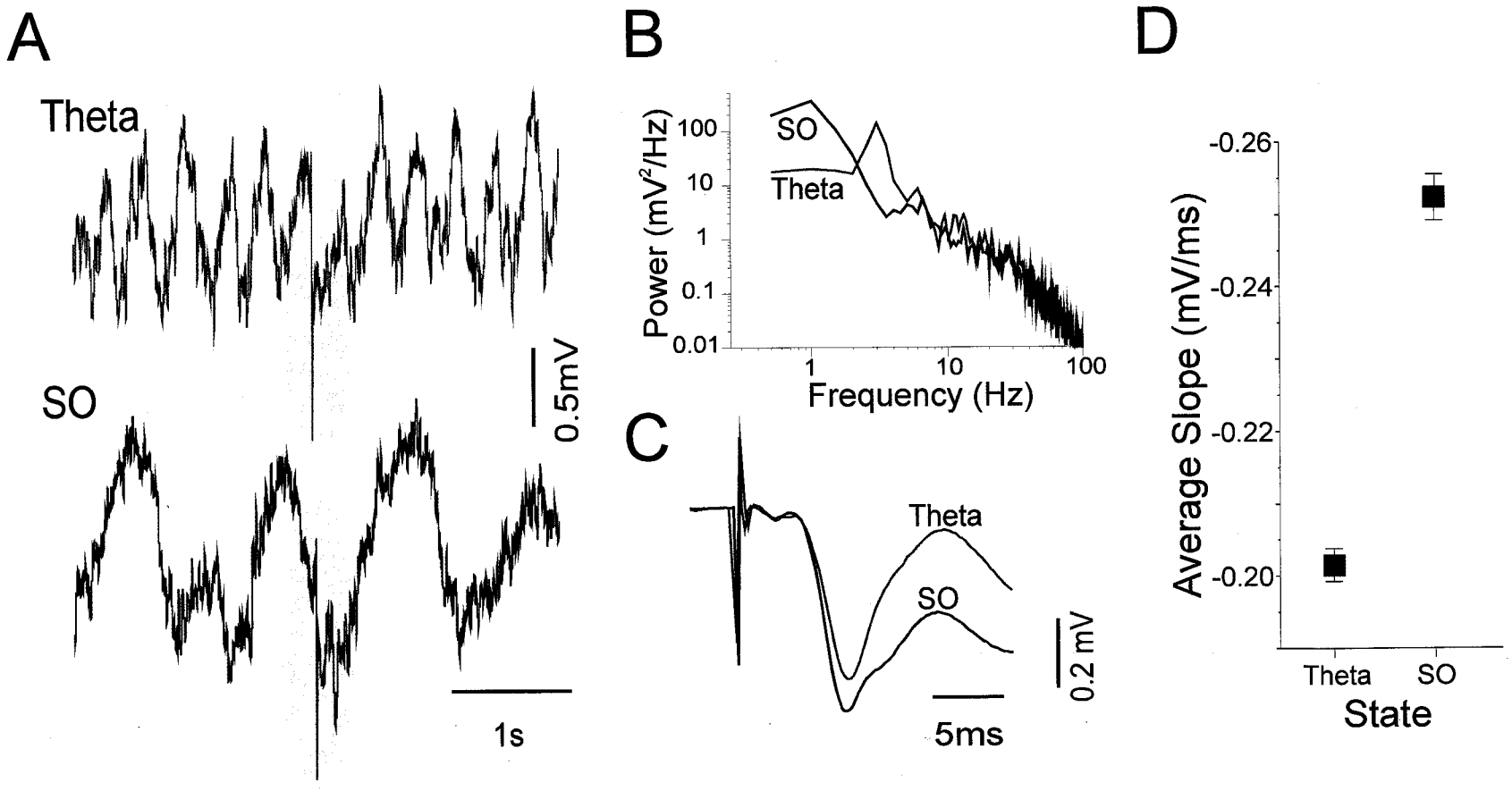
A
Theta
SO
0.5mV
1s
B
Power (mV²/Hz)
100
10
1
0.1
0.01
SO
Theta
1
10
100
Frequency (Hz)
C
Theta
SO
0.2 mV
5ms
D
Average Slope (mV/ms)
-0.26
-0.24
-0.22
-0.20
Theta
SO
State

Figure 2-4. Influence of State on CA3-CA1 Evoked Potentials. Average pEPSP slopes evoked during theta (filled squares), LIA (grey squares) and SO (hollow squares) are plotted as a normalized percentage of the average amplitude during theta. The pEPSP slopes evoked by CA3 stimulation were consistently and significantly higher during the SO and intermediate during LIA for each experiment and for the overall average across experiments.

Figure 2-4

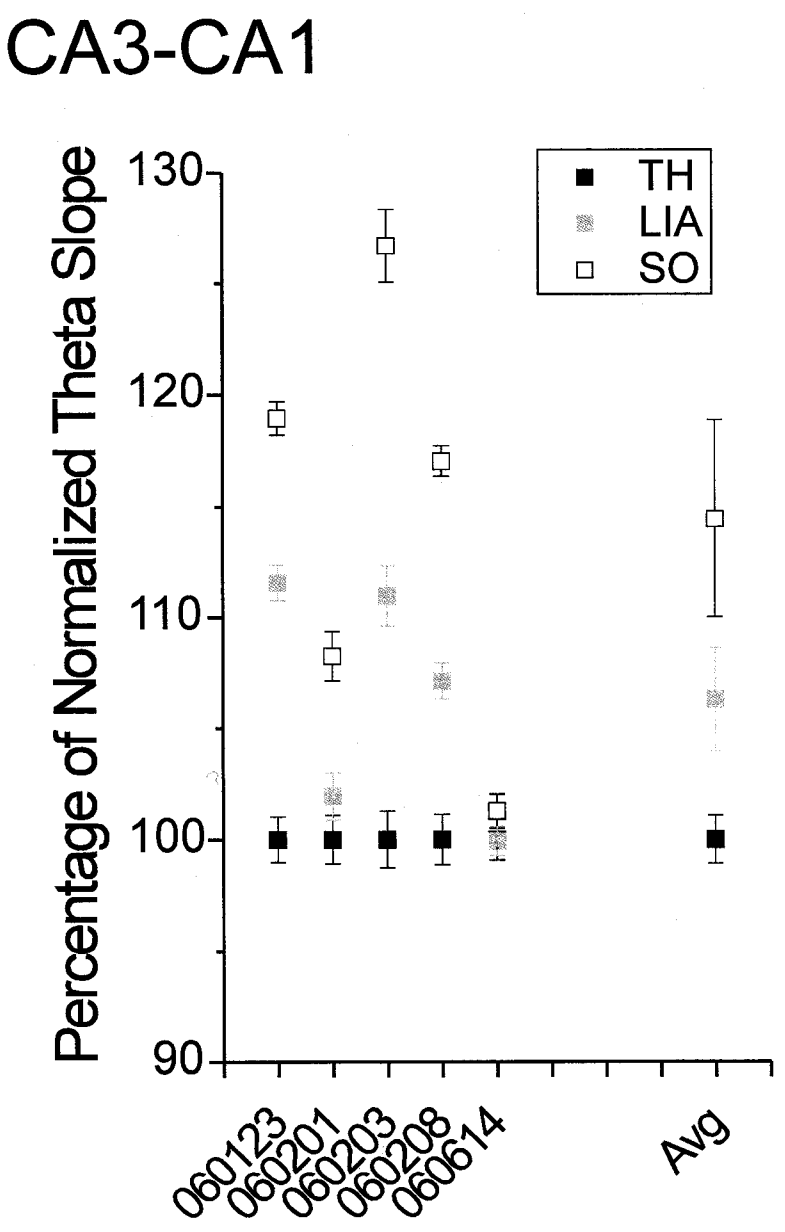
CA3-CA1
Percentage of Normalized Theta Slope
130
120
110
100
90
TH
LIA
SO
060123
060201
060203
060208
060614
Avg

Figure 2-5. Comparison of Current Source Density (CSD) in CA1. A 16 contact linear multiprobe was lowered into the HPC as shown in the diagram in **A)**. **B)** Average evoked potentials from the individual contact showing the largest field negativity following CA3 stimulation (2.8 mm depth – corresponding to stratum radiatum) are shown across both theta and the slow oscillation (SO) states. Dotted vertical lines denote the time point of maximum negativity in both examples and demonstrate the obvious increase in amplitude during the SO with respect to theta. **C)** CSD plots of the averaged evoked potential profile showed a larger amplitude sink at the level of stratum radiatum (see laminar diagram to right of plots) during the SO as compared to theta. **D)** Normalized averages of sink amplitudes across all (n=5) experiments. On average, the current sinks evoked at the level of stratum radiatum during the SO were larger than during theta.

Figure 2-5

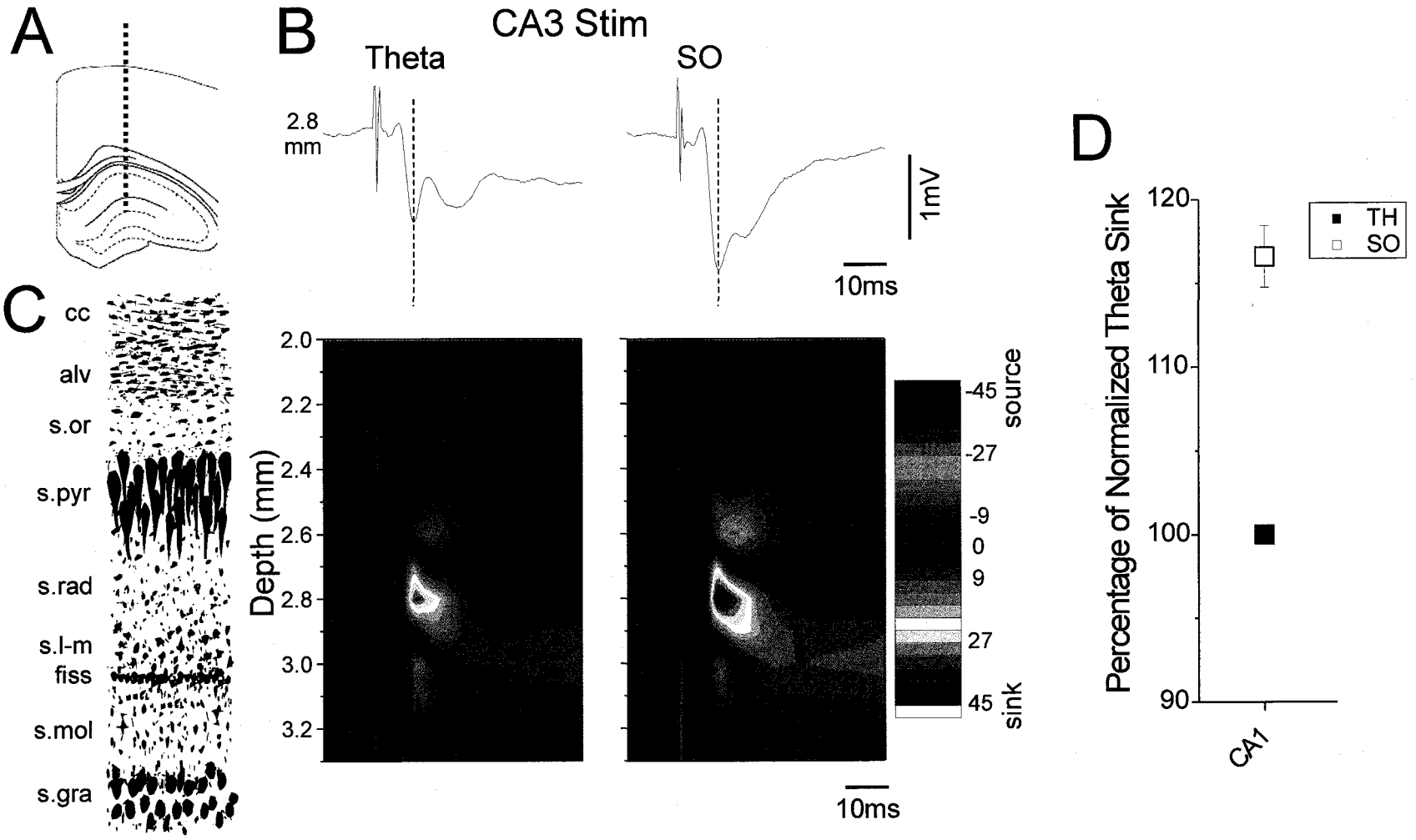
A
B
CA3 Stim
Theta
SO
2.8
mm
1mV
10ms
C
cc
alv
s.or
s.pyr
s.rad
s.l-m
fiss
s.mol
s.gra
Depth (mm)
2.0
2.2
2.4
2.6
2.8
3.0
3.2
-45
source
-27
-9
0
9
27
45
sink
10ms
D
Percentage of Normalized Theta Sink
120
110
100
90
TH
SO
CA1

Figure 2-6. Influence of State on PP-DG Evoked Potentials. Average pEPSP slopes evoked during theta (filled squares), LIA (grey squares) and SO (hollow squares) are plotted as a normalized percentage of the average amplitude during theta. The pEPSP slopes evoked by PP stimulation produced mixed results when compared across states. In two experiments the EPSP slopes were significantly lower while in the other three; they were significantly higher during the SO. Slopes during LIA tended to be intermediate.

Figure 2-6

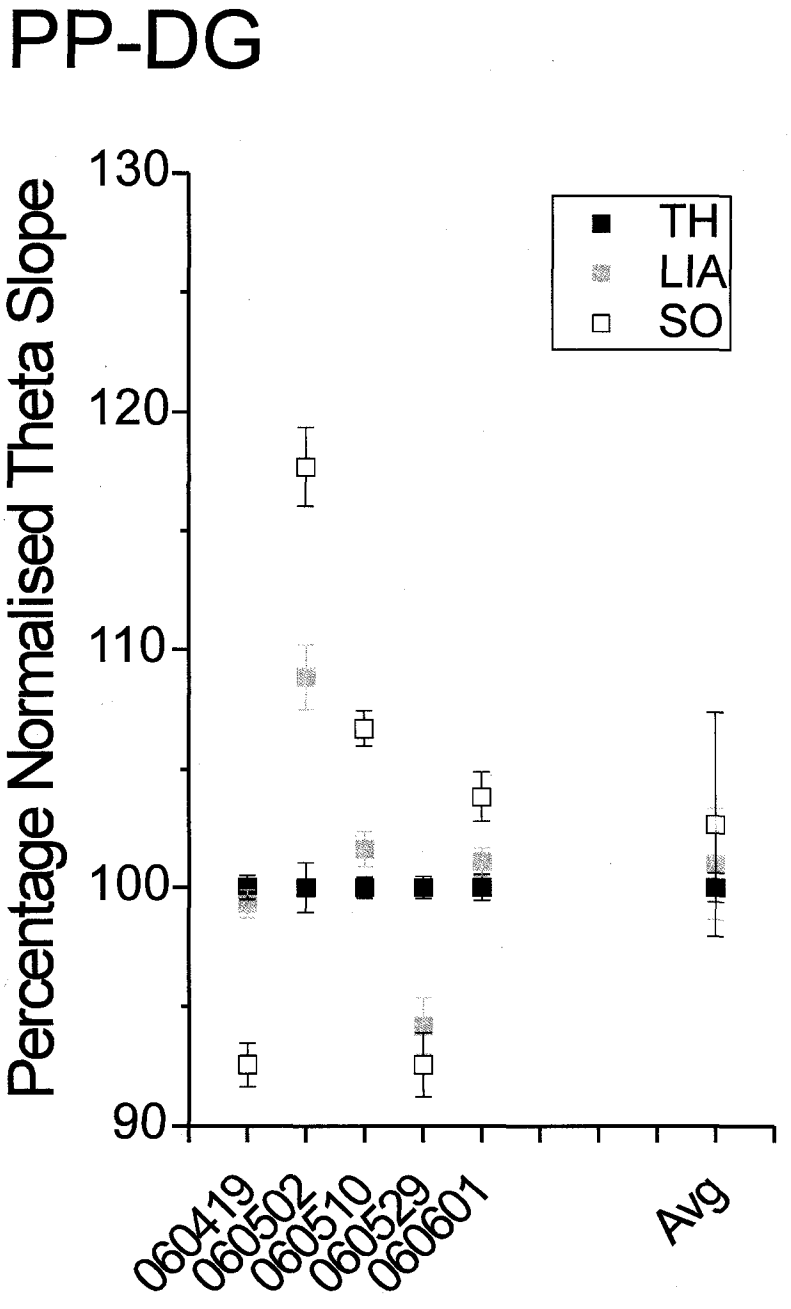
PP-DG
Percentage Normalised Theta Slope
130
120
110
100
90
TH
LIA
SO
060419
060502
060510
060529
060601
Avg

Figure 2-7. Influence of State on MPP, LPP and TA Evoked Potentials. Average EPSP slopes evoked during theta (filled squares), LIA (grey squares), and SO (hollow squares) expressed as a normalized percentage of the average amplitude during theta are plotted. **A)** Stimulation of the medial perforant path (MPP) elicited a smaller pEPSP slope during the SO as compared to theta in four out of five experiments and this difference was significant on average. No significant difference was observed between the average slopes across theta and LIA. **B)** Stimulation of the lateral perforant path (LPP) elicited a larger pEPSP slope during the SO as compared to theta in all experiments and this difference was significant on average. No significant difference was observed between the average slopes across theta and LIA. **C)** Stimulation of the temporal ammonic pathway (TA) elicited a larger pEPSP slope during the SO as compared to theta in all experiments and this difference was significant on average. Although slopes during LIA were consistently intermediate between theta and SO values, there was no significant difference on average between pEPSP slopes across theta and LIA.

Figure 2-7

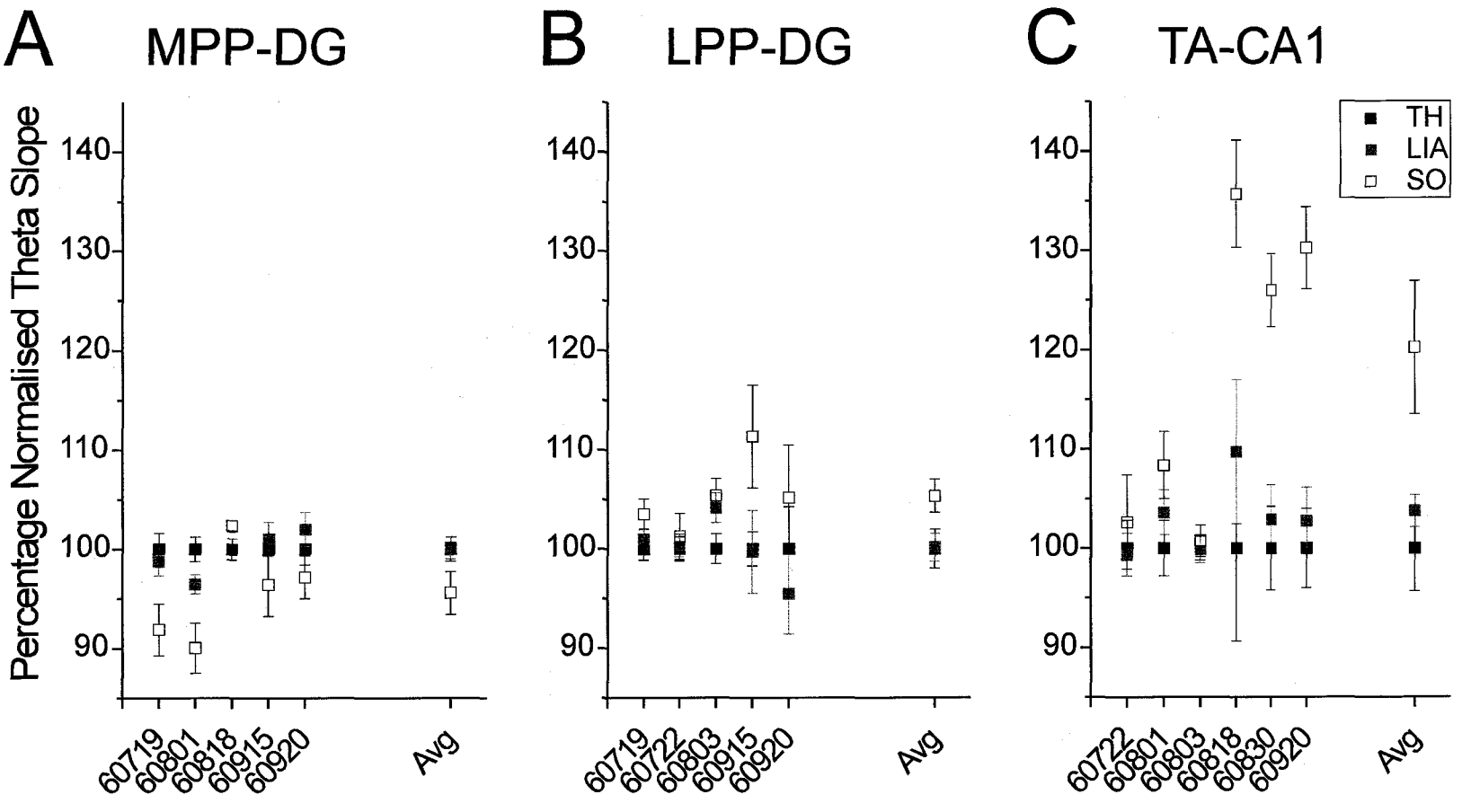
A
MPP-DG
B
LPP-DG
C
TA-CA1
Percentage Normalised Theta Slope
140
130
120
110
100
90
TH
LIA
SO
60719
60801
60818
60915
60920
Avg
60719
60722
60803
60915
60920
Avg
60722
60801
60803
60818
60830
60920
Avg

Figure 2-8. Comparison of Current Source Density (CSD) in DG. Data shown come from the same experiment illustrated in Figure 2-5. A 16 contact linear multiprobe was lowered into the HPC as shown in the diagram in **A**). **B)** Average evoked potentials from two separate contacts showing the largest field negativities corresponding to each respective pathway evoked by PP stimulation (3.2 and 3.1mm depths) are shown across both theta and the slow oscillation (SO) states. Dotted vertical lines highlight the respective components: MPP, LPP, and TA, respectively, in temporal order. Horizontal lines allow a comparison of the relative amplitudes of these components across states. Both LPP and TA showed increases during the SO while the MPP response was lower. **C)** CSD plots of the averaged evoked potential profile show a spatio-temporal dispersion of the sinks corresponding to the three components which are highlighted by labeled arrows. Sinks were larger for both the LPP and TA components and smaller for the MPP during the SO. **D)** Normalized averages of sink amplitudes across all experiments. On average, the current sinks corresponding to MPP stimulation were smaller, while those corresponding to either LPP or TA stimulation were higher during the SO.

Figure 2-8

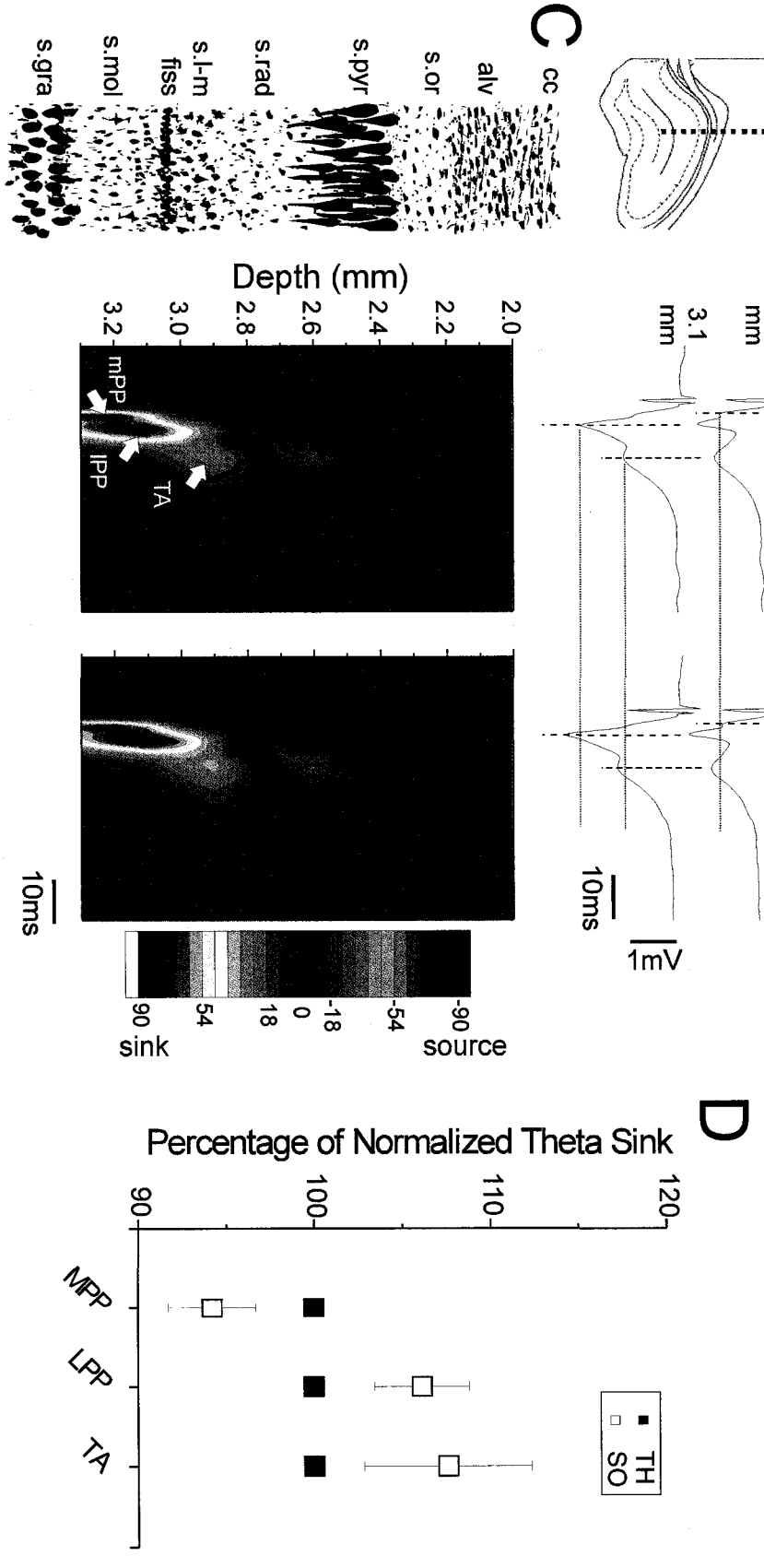
A
B
Theta
PP Stim
SO
3.2
mm
3.1
mm
10ms
1mV
C
cc
alv
s.or
s.pyr
s.rad
s.l-m
fiss
s.mol
s.gra
Depth (mm)
3.2
3.0
2.8
2.6
2.4
2.2
2.0
mPP
lPP
TA
10ms
90
54
18
0
-18
-54
-90
sink
source
D
Percentage of Normalized Theta Sink
90
100
110
120
MPP
LPP
TA
TH
SO

Figure 2-9. Phase-Dependent Modulation of Excitability. **A)** Examples of evoked potentials (EPs) in CA1 evoked by CA3 stimulation induced on the rising (top panel) and falling (bottom panel) phase of the ongoing theta cycle. The calculation of phase was estimated as illustrated by comparison to an idealized sinusoidal like function as illustrated by the overlays in red. **B)** The raw EPs for the traces shown in **A)** are superimposed at a faster sweep speed for comparison. The EP elicited on the falling phase of the theta cycle is substantially larger. **C)** Across all EPs evoked during theta in this experiment, the average pEPSP slope occurring on the falling phase was larger than the average pEPSP slope occurring on the rising phase.

Figure 2-9

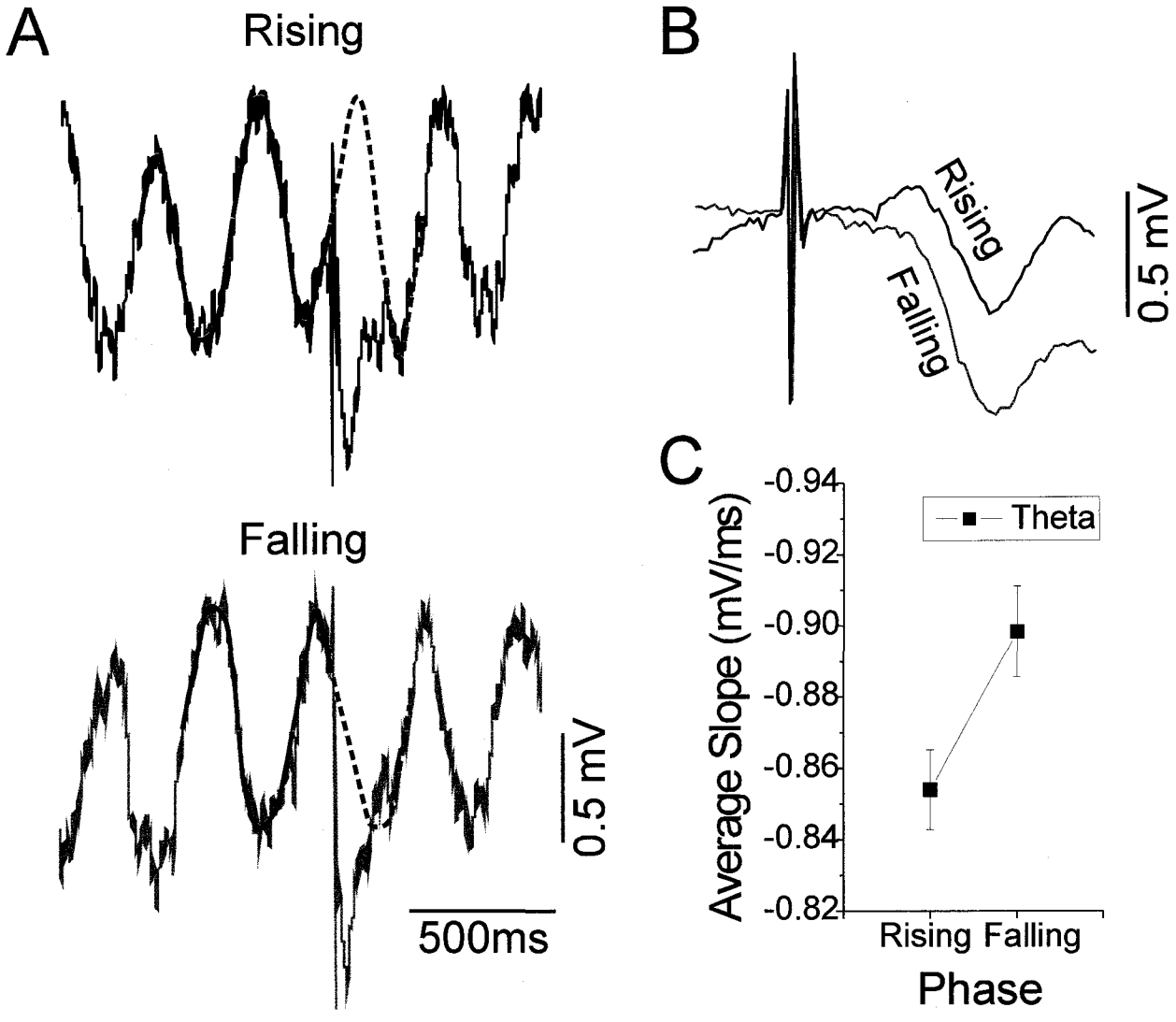
A
Rising
Falling
0.5 mV
500ms
B
Rising
Falling
0.5 mV
C
Theta
Average Slope (mV/ms)
-0.94
-0.92
-0.90
-0.88
-0.86
-0.84
-0.82
Rising Falling
Phase

Figure 2-10. Modulation of Excitability across Ongoing Rhythmic Cycles. Average normalized **A)** CA1 and **B)** DG pEPSP slope values following CA3 and PP stimulation, respectively, as a function of stimulation on differing oscillatory phases of theta or the SO. *i)* Slope values were significantly higher during the rising phase as compared to the falling phase for both theta (filled squares) and the slow oscillation (open squares) in **(A*i*)** CA1 and **(B*i*)** DG regions. *ii)* Polar plots of the phase angle at which the maximal slope occurred for every experiment in the **A*ii*)** CA1 and **B*ii*)** DG region (theta: filled circles slow oscillation: open circles). In every case except one, angles are clustered between 90 and 180 degrees, which corresponds to the first half of the falling phase of the respective oscillation. Average vectors across all experiments are also plotted as larger sized symbols and show a very tight distribution within the same quadrant. *iii*) Slope values were averaged across all experiments as a function of discrete bins and plotted during theta (filled squares) and the slow oscillation (open squares) for both the **A*iii*)** CA1 and **B*iii*)** DG regions. The superimposed sinusoidal grey waveform represents the field cycle at the appropriate phase for comparison. The delineation between rising and falling elements of the cycle is shown by the vertical line at 90 degrees while the delineation between the falling and rising elements of the cycle is shown by the vertical line at 270 degrees. Similar modulation is seen across both the theta and SO cycles and also in both CA1 and DG regions. The phase of maximum average synaptic excitability is noted by the closed (theta) and open (SO) arrowheads.

Figure 2-10

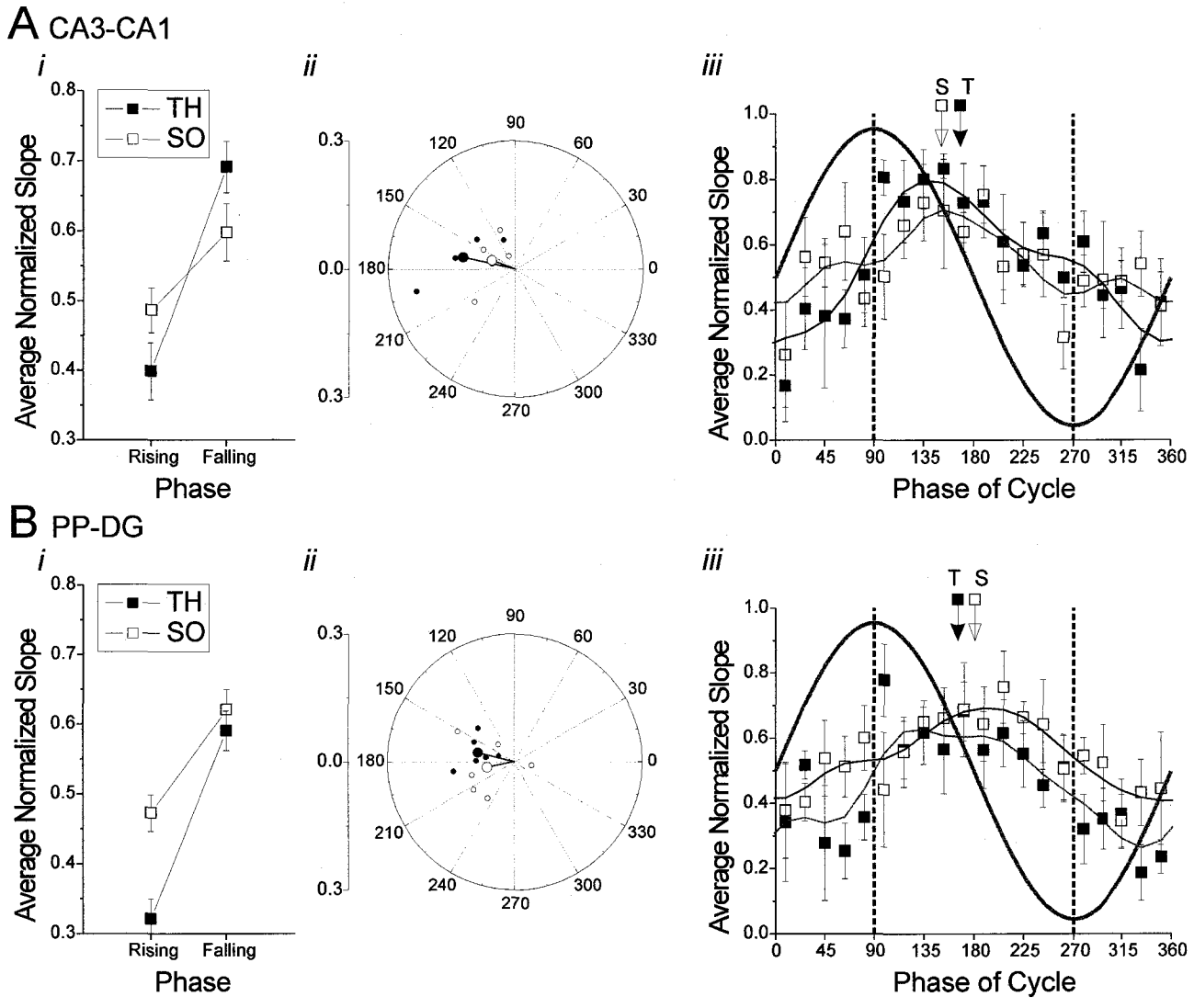
A CA3-CA1
i
ii
iii
TH
SO
Average Normalized Slope
Rising
Falling
Phase
S T
Phase of Cycle
B PP-DG
T S

References

Abraham WC and McNaughton N. Differences in synaptic transmission between medial and lateral components of the perforant path. *Brain Res* 303: 251-260, 1984.

Alonso A and Klink R. Differential electroresponsiveness of stellate and pyramidal-like cells of medial entorhinal cortex layer II. *J Neurophysiol* 70: 128-143, 1993.

Axmacher N, Mormann F, Fernandez G, Elger CE, and Fell J. Memory formation by neuronal synchronization. *Brain research reviews* 52: 170-182, 2006.

Bland BH. The physiology and pharmacology of hippocampal formation theta rhythms. *Prog Neurobiol* 26: 1-54, 1986.

Bodizs R, Bekesy M, Szucs A, Barsi P, and Halasz P. Sleep-dependent hippocampal slow activity correlates with waking memory performance in humans. *Neurobiology of learning and memory* 78: 441-457, 2002.

Born J, Rasch B, and Gais S. Sleep to remember. *Neuroscientist* 12: 410-424, 2006.

Bramham CR, Errington ML, and Bliss TV. Naloxone blocks the induction of long-term potentiation in the lateral but not in the medial perforant pathway in the anesthetized rat. *Brain Res* 449: 352-356, 1988.

Brun VH, Otnass MK, Molden S, Steffenach HA, Witter MP, Moser MB, and Moser EI. Place cells and place recognition maintained by direct entorhinal-hippocampal circuitry. *Science* 296: 2243-2246, 2002.

Buzsáki G. Hippocampal sharp waves: their origin and significance. *Brain Res* 398: 242-252, 1986.

Buzsáki G. Theta oscillations in the hippocampus. *Neuron* 33: 325-340, 2002.

Buzsáki G. Two-stage model of memory trace formation: A role for "noisy" brain states. *Neurosci* 31: 551-570, 1989.

Buzsáki G, Grastyan E, Czopf J, Kellenyi L, and Prohaska O. Changes in neuronal transmission in the rat hippocampus during behavior. *Brain Res* 225: 235-247, 1981.

Canning KJ and Leung LS. Lateral entorhinal, perirhinal, and amygdala-entorhinal transition projections to hippocampal CA1 and dentate gyrus in the rat: a current source density study. *Hippocampus* 7: 643-655, 1997.

Canning KJ, Wu K, Peloquin P, Kloosterman F, and Leung LS. Physiology of the entorhinal and perirhinal projections to the hippocampus studied by current source density analysis. *Annals of the New York Academy of Sciences* 911: 55-72, 2000.

Clement E, Thwaites M, Richard A, Ailon J, Peters S, and Dickson C. Sleep-like rhythmic alternations of brain state under urethane anesthesia. *Soc. Neurosci. Abstracts*. Society for Neuroscience, 2006, p. Program # 361.361.

Dahl D, Burgard EC, and Sarvey JM. NMDA receptor antagonists reduce medial, but not lateral, perforant path-evoked EPSPs in dentate gyrus of rat hippocampal slice. *Exp Brain Res* 83: 172-177, 1990.

Dahl D and Sarvey JM. Norepinephrine induces pathway-specific long-lasting potentiation and depression in the hippocampal dentate gyrus. *Proc Natl Acad Sci U S A* 86: 4776-4780, 1989.

Dickson C, Lo A, Clement E, and A R. Cyclical and sleep-like alternations of brain state under urethane anaesthesia. *Can J Neurol Sci* Suppl. 3 – S5: Program #9 B109 2007a.

Dickson C, Lo A, Clement E, Mah E, and Richard A. Cyclical and sleep-like alternations of brain state are specific to urethane anaesthesia. *Society for Neuroscience Abstracts*, 2007b, p. Program #791.793.

Eichenbaum H. Hippocampus: cognitive processes and neural representations that underlie declarative memory. *Neuron* 44: 109-120, 2004.

Eichenbaum H. Remembering: functional organization of the declarative memory system. *Curr Biol* 16: R643-645, 2006.

Ferbinteanu J, Holsinger RM, and McDonald RJ. Lesions of the medial or lateral perforant path have different effects on hippocampal contributions to place learning and on fear conditioning to context. *Behavioural brain research* 101: 65-84, 1999.

Foldvary-Schaefer N and Grigg-Damberger M. Sleep and epilepsy: what we know, don't know, and need to know. *J Clin Neurophysiol* 23: 4-20, 2006.

Fox SE. Membrane potential and impedance changes in hippocampal pyramidal cells during theta rhythm. *Exp Brain Res* 77: 283-294, 1989.

Freeman WJ. *Mass Action in the Nervous System*. New York: Academic Press, 1975.

Greenstein YJ, Pavlides C, and Winson J. Long-term potentiation in the dentate gyrus is preferentially induced at theta rhythm periodicity. *Brain Res* 438: 331-334, 1988.

Hahn TT, Sakmann B, and Mehta MR. Differential responses of hippocampal subfields to cortical up-down states. *Proc Natl Acad Sci U S A* 104: 5169-5174, 2007.

Hahn TT, Sakmann B, and Mehta MR. Phase-locking of hippocampal interneurons' membrane potential to neocortical up-down states. *Nat Neurosci* 9: 1359-1361, 2006.

Hargreaves EL, Rao G, Lee I, and Knierim JJ. Major dissociation between medial and lateral entorhinal input to dorsal hippocampus. *Science* 308: 1792-1794, 2005.

Harris KD, Henze DA, Hirase H, Leinekugel X, Dragoi G, Czurko A, and Buzsaki G. Spike train dynamics predicts theta-related phase precession in hippocampal pyramidal cells. *Nature* 417: 738-741, 2002.

Herman ST, Walczak TS, and Bazil CW. Distribution of partial seizures during the sleep--wake cycle: differences by seizure onset site. *Neurology* 56: 1453-1459, 2001.

Herreras O, Solis JM, Munoz MD, Martin del Rio R, and Lerma J. Sensory modulation of hippocampal transmission. I. Opposite effects on CA1 and dentate gyrus synapsis. *Brain Res* 461: 290-302, 1988.

Holscher C, Anwyl R, and Rowan MJ. Stimulation on the positive phase of hippocampal theta rhythm induces long-term potentiation that can be depotentiated by stimulation on the negative phase in area CA1 in vivo. *J Neurosci* 17: 6470-6477, 1997.

Hyman JM, Wyble BP, Goyal V, Rossi CA, and Hasselmo ME. Stimulation in hippocampal region CA1 in behaving rats yields long-term potentiation when delivered to the peak of theta and long-term depression when delivered to the trough. *J Neurosci* 23: 11725-11731, 2003.

Isomura Y, Sirota A, Ozen S, Montgomery S, Mizuseki K, Henze DA, and Buzsaki G. Integration and segregation of activity in entorhinal-hippocampal subregions by neocortical slow oscillations. *Neuron* 52: 871-882, 2006.

Jensen O and Lisman JE. Hippocampal sequence-encoding driven by a cortical multi-item working memory buffer. *Trends Neurosci* 28: 67-72, 2005.

Ji D and Wilson MA. Coordinated memory replay in the visual cortex and hippocampus during sleep. *Nat Neurosci* 10: 100-107, 2007.

Johnston D and Wu SM-s. *Foundations of cellular neurophysiology.* Cambridge, MA: MIT Press, 1995.

Ketchum KL and Haberly LB. Synaptic events that generate fast oscillations in piriform cortex. *J Neurosci* 13: 3980-3985, 1993.

Kloosterman F, van Haeften T, and Lopes da Silva FH. Two reentrant pathways in the hippocampal-entorhinal system. *Hippocampus* 14: 1026-1039, 2004.

Leung LS. Behavior-dependent evoked potentials in the hippocampal CA1 region of the rat. I. Correlation with behavior and EEG. *Brain Res* 198: 95-117, 1980.

Leung LS, Roth L, and Canning KJ. Entorhinal inputs to hippocampal CA1 and dentate gyrus in the rat: a current-source-density study. *J Neurophysiol* 73: 2392-2403, 1995.

Leung LW. Spectral analysis of hippocampal EEG in the freely moving rat: effects of centrally active drugs and relations to evoked potentials. *Electroencephalogr Clin Neurophysiol* 60: 65-77, 1985.

Marshall L, Helgadottir H, Molle M, and Born J. Boosting slow oscillations during sleep potentiates memory. *Nature* 444: 610-613, 2006.

McNaughton BL. Evidence for two physiologically distinct perforant pathways to the fascia dentata. *Brain Res* 199: 1-19, 1980.

Mehta MR, Lee AK, and Wilson MA. Role of experience and oscillations in transforming a rate code into a temporal code. *Nature* 417: 741-746, 2002.

O'Keefe J and Recce ML. Phase relationship between hippocampal place units and the EEG theta rhythm. *Hippocampus* 3: 317-330, 1993.

Pavlides C, Greenstein Y, Grudman M, and Winson J. Long-term potentiation in the dentate gyrus is induced preferentially on the positive phase of theta-rhythm. *Brain Res* 439: 383-387, 1988.

Penttonen M, Kamondi A, Acsady L, and Buzsáki G. Gamma frequency oscillation in the hippocampus of the rat: intracellular analysis *in vivo*. *Eur J Neurosci* 10: 718-728, 1998.

Rasch B, Buchel C, Gais S, and Born J. Odor cues during slow-wave sleep prompt declarative memory consolidation. *Science* 315: 1426-1429, 2007.

Remondes M and Schuman EM. Role for a cortical input to hippocampal area CA1 in the consolidation of a long-term memory. *Nature* 431: 699-703, 2004.

Robinson TE, Kramis RC, and Vanderwolf CH. Two types of cerebral activation during active sleep: relations to behavior. *Brain Res* 124: 544-549, 1977.

Rodriguez R and Haberly LB. Analysis of synaptic events in the opossum piriform cortex with improved current source-density techniques. *J Neurophysiol* 61: 702-718, 1989.

Rudell AP and Fox SE. Hippocampal excitability related to the phase of theta rhythm in urethanized rats. *Brain Res* 294: 350-353, 1984.

Rudell AP, Fox SE, and Ranck JB. Hippocampal excitability phase-locked to the theta rhythm in walking rats. *Exp Neurol* 68: 87-96, 1980.

Segal M. A correlation between hippocampal responses to interhemispheric stimulation, hippocampal slow rhythmic activity and behaviour. *Electroencephalogr Clin Neurophysiol* 45: 409-411, 1978.

Squire LR. Memory and the hippocampus: a synthesis from findings with rats, monkeys, and humans. *Psychol Rev* 99: 195-231, 1992.

Steriade M, Nunez A, and Amzica F. A novel slow (< 1 Hz) oscillation of neocortical neurons in vivo: depolarizing and hyperpolarizing components. *J Neurosci* 13: 3252-3265, 1993.

Suzuki SS and Smith GK. Spontaneous EEG spikes in the normal hippocampus. I. Behavioral correlates, laminar profiles and bilateral synchrony. *Electroencephalogr Clin Neurophysiol* 67: 348-359, 1987.

Tahvildari B and Alonso A. Morphological and electrophysiological properties of lateral entorhinal cortex layers II and III principal neurons. *J Comp Neurol* 491: 123-140, 2005.

Vanderwolf CH. Hippocampal electrical activity and voluntary movement in the rat. *Electroencephalogr Clin Neurophysiol* 26: 407-418, 1969.

Vanderwolf CH, Kramis R, and Robinson TE. Hippocampal electrical activity during waking behaviour and sleep: analyses using centrally acting drugs. *Ciba Found Symp*: 199-226, 1977.

Walker MP and Stickgold R. Sleep-dependent learning and memory consolidation. *Neuron* 44: 121-133, 2004.

Winson J and Abzug C. Neuronal transmission through hippocampal pathways dependent on behavior. . *J Neurophysiol* 41: 716-732, 1978.

Witter MP, Wouterlood FG, Naber PA, and Van_Haeften T. Anatomical organization of the parahippocampal-hippocampal network. *Annals of the New York Academy of Sciences* 911: 1-24, 2000.

Wolansky T, Clement EA, Peters SR, Palczak MA, and Dickson CT. The hippocampal slow oscillation: A novel EEG state and its coordination with ongoing neocortical activity. *J Neurosci* 26: 6213-6229, 2006.

Wyble BP, Linster C, and Hasselmo ME. Size of CA1-evoked synaptic potentials is related to theta rhythm phase in rat hippocampus. *J Neurophysiol* 83: 2138-2144, 2000.

Ylinen A, Bragin A, Nadasdy Z, Jando G, Szabo I, Sik A, and Buzsaki G. Sharp wave-associated high-frequency oscillation (200 Hz) in the intact hippocampus: network and intracellular mechanisms. *J Neurosci* 15: 30-46, 1995a.

Ylinen A, Soltesz I, Bragin A, Penttonen M, Sik A, and Buzsáki G. Intracellular correlates of hippocampal theta rhythm in identified pyramidal cells, granule cells, and basket cells. *Hippocampus* 5: 78-90, 1995b.

Yun SH, Mook-Jung I, and Jung MW. Variation in effective stimulus patterns for induction of long-term potentiation across different layers of rat entorhinal cortex. *J Neurosci* 22: RC214, 2002.

Zar JH. *Biostatistical Analysis*. Upper Saddle River, NJ.: Prentice Hall Inc., 1999.

Chapter 3: Cholinergic Manipulations

Introduction

The regulation of declarative memories, a term encompassing all memories that require a conscious effort during recall, is associated with the activity of the hippocampus (HPC) (Eichenbaum 2004; Scoville and Milner 1957; Squire 1992). In addition to hippocampal activity exhibited during awake learning sessions, the pattern hippocampal activity during the subsequent sleep periods following the learning event have also been identified as playing an important role in the proper development and preservation of memories (Plihal and Born 1997; Stickgold 2005). As such, efforts to increase our understanding of how memory works have become closely linked to studying the properties of the HPC during all behavioral states, including sleep.

EEG recordings taken from the HPC reveal that during natural sleep, as well as under urethane anesthesia, the HPC spontaneously alternates through several distinguishable activity states including two highly rhythmic patterns, the 3 to 12 Hz theta rhythm (Bland 1986) and the recently discovered 1 Hz slow oscillation (SO) (Wolansky et al. 2006). The HPC also engages in periods of a non-rhythmic activity pattern called large-amplitude irregular activity (LIA) which occurs in the transition period between the two rhythmic states. The state alternations occurring in the HPC are correlated with specific stages of sleep (theta during REM and LIA and SO during nonREM) (Bland 1986; Wolansky et al. 2006) and are proposed to underlie different functions in memory processing and consolidation (Buzsáki 1989; Wolansky et al. 2006).

The field oscillations observed in the HPC represent fluctuations in the membrane potentials of networks of neurons. These synchronized rhythmic states can influence

synaptic activity within the HPC by providing differential modulation across states in addition to a temporal processing constraint within each state. Changing the activity state of the HPC alters the network dynamics at a given point in time, producing changes in the way the synapses respond and ultimately influencing the way the HPC processes information. Previous studies have shown that hippocampal synaptic responses are altered as a function of the theta and LIA states during both awake behavior (Buzsáki et al. 1981; Leung 1980; Segal 1978) and under urethane (Leung 1985).

In a recent study we were able to take the analysis of state one step further by including a comparison of SO in addition to that of theta and LIA in rats under urethane anesthesia (Schall et al. 2007). We also took into consideration variations of synaptic excitability across hippocampal subregions by examining a variety of pathways within the hippocampus. These included the terminals of CA3 and temporal ammonic (TA) pathways in CA1 as well as the terminals of the medial perforant path (MPP), and the lateral perforant path (LPP) in the dentate gyrus (DG). We found that state produced a significant modulation of synaptic excitability at each of the terminal sites we examined in the HPC with the largest response differences existing between theta and SO. In CA1, the CA3 and the TA synaptic responses were always larger during periods of SO and this was also the finding for the LPP responses in the DG. However, the MPP response in the DG was greatest during theta, indicating that hippocampal region and state interact to provide a system capable of variable responses suited for the complex processing of declarative memory formation and consolidation attributed to the HPC.

It is known that the theta activity produced during sleep and under urethane anesthesia is modulated by cholinergic mechanisms (Bland 1986; Vanderwolf 1988).

Wolansky et al. (2006) showed that the SO observed in sleeping and urethane anesthetized rats is also modulated by cholinergic activity. The application of a cholinergic agonist induced theta while injections of cholinergic antagonists promoted SO (Wolansky et al. 2006). Given the documented relationship between cholinergic activity and hippocampal state in addition to the relationship between hippocampal state and synaptic excitability we wanted to examine whether hippocampal states produced by cholinergic manipulations would initiate synaptic responses comparable to those found across spontaneously occurring states. To investigate this, rats were anesthetized with urethane and evoked potentials were elicited and recorded during spontaneous theta and SO as well as during cholinergically manipulated periods of theta and SO. We found that responses generated during the cholinergic manipulations were equivalent and in some cases enhanced beyond their normal modulation with spontaneous occurring states. Therefore it appears that changes in the synaptic excitability of hippocampal circuits across states is determined by both direct and indirect cholinergic neuromodulatory effects. These results have profound implications for hippocampal processing during the alternating stages of REM and nonREM sleep.

Materials and Methods

Data were obtained from 25 male Sprague Dawley rats weighing 184 to 512 g (average ± SEM: 313.52 ± 15.47 g). All methods used conformed to the guidelines established by the Canadian Council on Animal Care and the Society for Neuroscience and were approved by the Biosciences Animal Policy and Welfare Committee of the University of Alberta.

Surgical, implantation, recording and stimulating procedures

Animals were initially induced with gaseous isoflurane mixed with medical O_2 at a minimum alveolar concentration (MAC) of 4 in an enclosed anaesthetic chamber. After loss of righting reflexes, they were maintained on isoflurane (2.0-2.5 MAC) via a nose cone and implanted with a jugular catheter. Isoflurane was discontinued, and general anesthesia was achieved using slow intravenous administration of urethane (0.8 g/ml; final dosage, 1.8 ± 0.03 g/kg) via the jugular vein. Body temperature was maintained at 37°C using a servo-driven system connected to a heating pad and rectal probe (TR-100; Fine Science Tools, Vancouver, BC, Canada) for the remainder of the surgical and recording procedures. Level of anesthesia was assessed throughout the experiment by monitoring reflex withdrawal to a hind paw pinch. If any visible withdrawal occurred, the animal was administered a supplemental dose (0.01 ml) of urethane.

When the rats no longer exhibited a withdrawal reflex they were moved to a stereotaxic apparatus for electrode placement. Stereotaxic coordinates were calculated from bregma and respective holes were drilled in the skull to allow electrode penetration in the brain. A 16 contact linear multiprobe (100μm spacing: Neuronexus Technologies, Ann Arbour, MI) was implanted to span the pyramidal layer of area CA1 to the molecular layer of the dentate gyrus (DG) (AP, -3.3; ML, ±1.8 to ±2.1; DV, -2.7 to 3.5). These placements were optimized for commissural and perforant path stimulation, respectively (see further below).

For recordings from CA1, evoked potentials (EP) were elicited by stimulating the contra lateral CA3 area using an implanted bipolar electrode constructed from two twisted teflon-insulated stainless steel wires (110 μm bare diameter) at the following

coordinates (AP, -3.5; ML, -3.5; DV, -3.0 to -4.0). DG responses were recorded by stimulation of the ipsilateral perforant pathway (PP) (AP, -7.0; ML, -4.0 to -5.5; DV, -1.5 to –2.5) using an identical electrode. Stimulation was conducted using a 0.2 millisecond biphasic current pulse at an intensity range of 40 to 240 μA using an isolated constant current pulse generator (model 2100; A-M Systems, Carlsborg, WA). The stimulation electrodes were adjusted in the vertical plane to ensure a maximal response.

Signals from the probe were referenced to ground (stereotax) and amplified at a final gain of 1000 and wide-band filtered between 0.5 and 10 kHz via a 16-channel head stage (unity gain) and amplifier system (Plexon, Dallas, TX). All signals were low pass filtered at 500 Hz and then digitized with a Digidata 1322A A-D board connected to a Pentium PC running the AxoScope acquisition program (Molecular Devices; Union City, CA). Signals were sampled at 1 kHz or above and were digitized online.

Experimental Procedure

After suitable sites were located the experimental procedure began with the collection of a 10 to 20 minute recording of spontaneous activity for verification of state alternations. Following the acquisition of baseline spontaneous recordings, two independent samples of the EP profiles elicited during periods of theta and SO activity were taken. Each sample consisted of at least 16 traces, during which EPs were generated at a rate between 6 to 9 seconds. For data collected from stimulation of the PP, paired pulse profiles at an interpulse interval of 50 msec were also collected during states of theta and SO for the analysis of paired pulse depression or facilitation, used to determine the classification of MPP and LPP EPs, respectively

Once samples during spontaneous theta and SO had been successfully collected the rat was then administered a cholinergic agonist and/or antagonist to induce periods of prolonged theta and SO activity, respectively. To stimulate theta activity the rat was injected intravenously with either oxotremorine (n=1) or eserine (n=14). Injections were conducted very slowly with small bolus amounts (0.05ml) separated by one to two minutes. During injections a continuous recording was taken, during which the spontaneous EEG was monitored. A cholinergic-induced theta state was determined to take place when no state changes into deactivated patterns (LIA or SO) took place over an entire alternation time cycle (11.37 ± 0.7 minutes). If deactivated patterns were detected the rat was given an additional 0.05 ml dose of the agonist, which was repeated until the EEG showed continuous theta for an entire cycle time period. Once the rat was in a stable and continuous state of theta, at least two samples of the EP profile were collected as described above. One sample was always taken from a time frame during which deactivated patterns were expected to occur based on the timing of the alternations occurring prior to the cholinergic manipulation. This ensured that the data was collected during theta that was cholinergically, and not spontaneously, induced.

The cholinergic antagonist was given after the agonist samples had been collected or in some cases after the theta and SO samples in some experiments where an agonist sample was not required. Atropine (n=10) or scopolamine (n=8) injections were given i.p. to initiate an uninterrupted deactivated state. During the administration of the cholinergic antagonist a continuous recording was taken to monitor the ongoing EEG activity. Similar to the case of the agonist, but in reverse, a cholinergic manipulated state of SO activity was determined by the absence of any theta activity over a time frame

during which an alternation of state was expected to take place. If theta activity did occur, a second supplemental dose (10% of original) was administered and the process was repeated until theta was continuously absent. Two samples of the EP profile were collected as described above, ensuring that one coincided with a time frame during which activated (theta) patterns were expected to occur based on the timing of the alternations occurring prior to the drug administration.

Following recording sessions, a small lesion was made at the tip of all stimulating electrodes by passing 1 mA of DC current for 5 seconds using an isolated constant current pulse generator (model 2100; A-M Systems). To make the multiprobe track visible for histological purposes, the probe was moved slightly in two horizontal planes at its most ventral position.

Histological Procedure

Rats were perfused transcardially, initially with physiological saline then with 4% Para formaldehyde in saline. Brains were extracted and stored overnight in 30% sucrose in 4% Para formaldehyde. The tissue was frozen with compressed CO_2 and sliced at 60 μm with a rotary microtome (1320 Microtome; Leica, Vienna, Austria). Slices were then mounted on gel-coated slides, allowed to dry for a minimum of 24 h, subsequently stained using thionin and cover slipped. Microscopic inspection of stained slices was used to verify recording loci. Digital photomicrographs (Canon Powershot S45; Canon, Tokyo, Japan) were taken on a Leica DM LB2 microscope, imported using Canon Remote Capture 2.7 software and processed with Corel PhotoPaint (Corel, Ottawa, Ontario, Canada).

Data Analysis

Current source density

Current source density (CSD) analysis was conducted on spontaneous and averaged field potential profiles recorded using the linear multiprobe following the assumptions of (Freeman 1975; Ketchum and Haberly 1993; Rodriguez and Haberly 1989). Briefly, CSD was computed by estimating the second spatial derivative of unfiltered voltage traces derived from the multiprobe. This estimate was calculated using a three-point difference (differentiation grid size of 300 μm) on the voltage values across spatially adjacent traces:

$$CSD = [f(p_{i-1})-2f(p_i)+f(p_{i+1})]/d^2 \qquad \text{(Equation 1)}$$

Where $f(p_i)$ is the field signal from probe channel i ($i = 2, 3, \ldots, 14$) and d is the distance between adjacent channels (0.1mm). For probe traces at both ends of the probe (channels 1 and 16) the differentiation grid was based only on the immediately adjacent channel (2 and 15, respectively). We confirmed that this procedure yielded similar, if not identical, CSD results as the 3 point differentiation method by successively eliminating probe end channels and then recomputing and comparing the results.

Comparison between States

Samples containing 16 traces of the EP profile were obtained during periods of spontaneous theta, spontaneous SO, cholinergic agonist induced theta and cholinergic antagonist induced SO. An average profile was generated from the 16 traces and used to construct a CSD plot. From the CSD plot a maximum sink value was obtained for each state. Within an experiment all sink values were standardized to those observed during

theta by dividing each value by the theta value and multiplying by 100 so that each state value was now expressed as a percentage with theta serving as a benchmark at 100 percent.

Data summary and statistics

Arithmetic averages were computed between experiments and were reported together with the standard error of the mean (SEM). A one factor, four level ANOVA was conducted to test for an overall difference between the average sinks values of the theta, SO, agonist and antagonist conditions. Following a significant F value, planned comparisons were carried out between conditions of interest using t-tests. Comparisons between theta and SO, theta and the antagonists as well as SO and the agonists were evaluated through one-tailed paired sample t-tests. Comparisons between the agonist and antagonist conditions were conducted using one-tailed independent sample t-tests as the condition averages contained values from different experiments. All tests used an alpha (probability) level of 0.05.

Drugs and chemicals

Oxotremorine and eserine salicylate salt were applied iv to produce elongated periods of theta activity. Oxotremorine was mixed with saline at a concentration of 10 mg/ml and administered to a final dose of 2.82 mg/kg. Eserine was mixed with saline at a concentration of 4 mg/ml and administered to a final dose of 0.71 ± 0.1 mg/kg. Atropine sulphate salt hydrate and scopolamine hydrobromide were injected ip to elicit extended periods of SO activity. Atropine was mixed with saline at a concentration of 50 mg/ml and administered to a final dose of 55.79 ± 4.97 mg/kg. Scopolamine was mixed with

saline at a concentration of 5 mg/ml and administered to a final dose of 18.73 ± 2.06. All drugs were obtained from Sigma.

Results

Histological findings

We confirmed the location of all multiprobe and stimulating electrode locations. Multiprobe tracts were all in a plane that traversed the CA1 pyramidal cell layer, through the hippocampal fissure and the DG. The termination of probe tracts was typically in stratum granulosum or in the hilar region of the DG just ventral to the granule cell layer. The position of individual contact sites was estimated from the position of the histological tract in combination with comparisons to the distribution of spontaneous (theta and SO) and evoked potential profile measures (Wolansky et al. 2006). Stimulation sites in the contra-lateral CA region were in or near CA3. These sites could be close to the lower blade of the CA3 pyramidal layer, in the mid-apical dendritic zone of stratum radiatum of CA3 at the level of its vertical curvature or in stratum radiatum close to the CA1/CA3 border. Stimulation sites aimed at the PP were found to be in or just superior to the dorsal element of the angular bundle. Summary placements and tracks for all experiments are shown in Figure 3-1.

Analysis of Spontaneous and Cholinergic Modulated State

As previously described (Wolansky et al. 2006) the activity of the HPC spontaneously alternated between activated (theta), transition (large amplitude irregular activity: LIA), and deactivated (SO) patterns. Our analysis focused on the states of theta and SO since a) previous results we have obtained suggest the largest difference in

synaptic activity occurs between these states (Schall et al. 2007) and b) the activity present during theta and SO were predicted to be comparable to that observed after application of the cholinergic agonists and antagonists, respectively (Wolansky et al. 2006). Spontaneous theta was characterized by a rhythmic pattern with an average frequency of 3.87 ± 0.13 Hz (Figure 3-2). Spontaneous periods of SO were comprised of large, rhythmic waves at an average frequency of 1.23 ± 0.15 Hz (Figure 3-2).

Administration of cholinergic agonists reliably produced a prolonged period of theta activity that was maintained even across time periods in which normal alterations to deactivated states should have occurred. Although the effect of the cholinergic agonist was detectable by visual inspection, frequency analysis was carried out to confirm that activity following the administration of the agonist was within the theta frequency bandwidth. Activity following the injection of oxotremorine or eserine was similar to that observed during spontaneous theta and exhibited an average frequency of 3.54 ± 0.18 (Figure 3-2).

Application of the cholinergic antagonist produced a reliable and long lasting period of SO activity which was maintained across time periods during which normal alternations to the activated state should have occurred. The activity observed after the injection of atropine or scopolamine was visually comparable to that recorded during SO but frequency analysis was utilized to ensure that the activity was within the frequency bandwidth typically associated with SO. Activity following application of the cholinergic antagonist showed an average frequency of 0.91 ± 0.04 Hz (Figure 3-2).

Evoked potential and CSD profile comparisons

CA3 – CA1

EP profiles evoked by contra lateral CA3 stimulation showed a maximum negativity occurring at the level of stratum radiatum as matched to spontaneous activity profiles (just below the point of theta amplitude minimum and phase reversal) (Schall et al. 2007; Wolansky et al. 2006) (Figure 3-3). The EP traces recorded directly at this maximum level were similar to pEPSPs as previously described for CA3 inputs (Schall et al. 2007; Wyble et al. 2000). They exhibited a maximum negative peak at a latency of 12.62 ± 1.12 ms post-stimulation.

CSD profiles calculated from the above were also similar to those described for stimulation of CA3 inputs (Schall et al. 2007; Wolansky et al. 2006). A maximal sink matching to both the location and timing of the maximal voltage negativity was observed. As previously shown, this sink was consistently larger during SO than theta (Schall et al. 2007) and was also enhanced during treatments with cholinergic antagonists as opposed to cholinergic agonists (Figure 3-3).

The average normalized (to theta) CSD sink values in CA1 across all experiments were 122.29 ± 3.72 for SO (n = 10), 83.36 ± 7.45 for the cholinergic agonist (n = 7) and 119.50 ± 11.59 for the cholinergic antagonist (n = 7) (Figure 3-4). As shown in the example illustrated (Figure 3-4) the average amplitude of the peak sink during SO appeared larger than that observed during theta. As might be expected, the average sink at the same level and latency recorded during the agonist condition appeared smaller than that observed during the prolonged SO activity generated in the antagonist condition. In addition, the sink values obtained in the SO and antagonist conditions appeared to be

comparable while the agonist condition had a sink value which appeared to be even lower than that occurring during spontaneous theta (Figure 3-4).

The overall ANOVA between the four conditions was significant ($F(3,30) = 8.49$, $p = 0.00031$). Paired sample t-tests were then utilized to carry out comparisons of interest between spontaneous theta and SO, as well as spontaneous conditions versus their analogous and opposing cholinergically-induced counterparts. An independent sample t-test was used to test the difference between the theta condition evoked by cholinergic agonism versus the SO condition evoked by cholinergic antagonism as several samples came from different experiments. Corresponding to our previous findings (Schall et al. 2007), inward synaptic (sink) currents evoked by CA3 stimulation were significantly larger during SO then theta ($t(9) = -3.04$, $p = 0.007$). Correspondingly, there was also a significant difference between the sinks observed in the agonist and antagonist conditions ($t(12) = -2.62$, $p = 0.01114$), indicating that inward synaptic current was larger following cholinergic receptor antagonism. Furthermore, there was a significant enhancement of current sinks when comparing the spontaneous SO versus the cholinergic agonist conditions ($t(6) = -6.82$, $p = 0.00024$). Despite a trend for the sinks to be larger during the antagonist condition, they were not found to be significantly different from the spontaneous theta condition ($t(6) = -1.81$, $p = 0.05977$). The comparison of sinks between both the spontaneous and cholinergically-induced theta states ($t(6) = 0.91$, $p = 0.199$) and the spontaneous and cholinergic SO states ($t(6) = -0.17$, $p = 0.436$) were not significant.

MPP – DG

EP profiles evoked by stimulation of the perforant path which exhibited paired pulse depression and were located in the middle portion of the molecular layer of the DG (i.e. having maximum negativities ≥100μm below the point of maximum theta or SO amplitudes but above the DG granule cell layer) were classified as MPP (Schall et al. 2007) (see Figure 3-5). A total of ten experiments were found that could be classified as MPP responses and these showed an average paired pulse depression of 90.03 ± 2.34 percent. The EP traces recorded directly at the level of maximum negativity were similar to pEPSPs as previously described for MPP inputs to the DG with an average negative peak latency of 4.03 ± 0.10 ms, coinciding with previously established MPP latencies (Canning et al. 2000; Leung et al. 1995; Schall et al. 2007).

CSD plots calculated from these average EP profiles were also similar to those described for stimulation of MPP inputs to the DG (Schall et al. 2007). A maximal sink matching to both the location and timing of the maximal voltage negativity was observed. As shown, and in contrast to the CA3 to CA1 activation, this sink appeared larger during theta as opposed to the SO and was also enhanced during treatments with cholinergic agonists as opposed to cholinergic antagonists (Figure 3-5).

The average normalized (to theta) CSD sink values for MPP stimulation in the DG were 95.33 ± 1.86 (n = 10) for SO, 106.91 ± 3.66 (n = 5) for the agonist condition and 83.88 ± 6.56 (n = 6) for the antagonist condition (Figure 3-7). Thus, currents evoked by MPP stimulation showed the exact opposite trend from those evoked by CA3 stimulation in CA1 with larger responses generated during the theta and agonist conditions rather than the SO and antagonist conditions (Figure 3-7).

The overall ANOVA between the four conditions showed that there was a significant effect between the activity states ($F(3,27) = 7.86$, $p = 0.00063$). Follow up t-tests were conducted on comparisons of interest in the same manner as with previous data. As previously reported (Schall et al. 2007), the average sink generated during theta was significantly larger than it was during SO ($t(9) = 2.77$, $p = 0.01093$). In parallel, the comparison between the sink values evoked during the cholinergic agonist versus the antagonist conditions was also significant ($t(9) = 2.89$, $p = 0.00894$). Although the spontaneous theta and the SO condition evoked by cholinergic antagonists were not significantly ($t(5) = 1.75$, $p = 0.07005$), the spontaneous SO and the cholinergically-induced theta conditions were ($t(4) = -2.55$, $p = 0.03169$) . Differences between spontaneous activities and their equivalent conditions evoked by cholinergic agents were non-significant for both theta ($t(4) = -1.97$, $p = 0.060$) and SO ($t(5) = 1.18$, $p = 0.146$).

LPP – DG

EP profiles evoked by perforant path stimulation which exhibited paired pulse facilitation and were located in the upper portion of the molecular layer of the DG (i.e. having maximum negativities $\leq$100μm below the point of maximum theta or SO amplitudes but above the DG granule cell layer) were classified as LPP (Schall et al. 2007) (see Figure 3-6). Using this criteria there were a total of ten experiments that contained a LPP component, which showed an average facilitation of 115.13 ± 3.45 percent. The EP traces recorded directly at the level of maximum negativity were similar to pEPSPs as previously described for LPP inputs to the DG with an average peak latency of 4.96 ± 0.24 4.03 ± 0.10 ms to negative peak, coinciding with previously established

LPP latencies from other studies(Canning et al. 2000; Leung et al. 1995; Schall et al. 2007).

CSD plots calculated from these average EP profiles were also similar to those described for stimulation of LPP inputs to the DG (Schall et al. 2007). A maximal sink matching to both the location (the outermost portion of the stratum moleculare of the DG) and timing of the maximal voltage negativity in the EP was observed. As shown, and in contrast to the results for MPP activation, this sink appeared larger during the SO as opposed to theta and was also enhanced during treatments with cholinergic antagonists as opposed to cholinergic agonists (Figure 3-6).

The average normalized (to theta) CSD sink values for LPP stimulation in the DG were 109.50 ± 1.55 (n = 10) for SO, 85.44 ± 7.21 (n = 7) for the agonist condition and 113.01 ± 6.28 (n = 5) for the antagonist condition (Figure 3-7). This pattern of results followed the same trend as those for CA3 stimulation in CA1 exhibiting larger responses for spontaneous and cholinergic SO states compared to the spontaneous and cholinergic theta states (Figure 3-7).

The overall ANOVA for LPP means was significant ($F(3,28) = 9.16$, $p = 0.00022$) indicating reliable differences in the size of the sinks obtained across the activity states. The same series of t-tests conducted on CA1 and MPP data was used to evaluate comparisons of interest from the LPP data. As we have previously found (Schall et al. 2007), the synaptically evoked sink was significantly larger, on average, during spontaneous SO as compared to spontaneous theta ($t(9) = -4.91$, $p = 0.00042$). In parallel, the same comparison between the two cholinergically evoked state of SO and theta was also significant ($t(10) = -2.73$, $p = 0.01056$), with larger sinks appearing during SO

evoked by the muscarinic antagonists. Sinks evoked during spontaneous SO as compared to agonist induced theta were significantly larger ($t(6) = 3.15$, $p = 0.00985$), although those evoked during antagonist-induced SO as compared to spontaneous theta were not ($t(4) = -2.06$, $p = 0.05411$). There were no significant differences in the magnitude of the sinks elicited during spontaneous and cholinergically induced theta ($t(6) = 1.43$, $p = 0.101$) or spontaneous and induced SO ($t(4) = -1.11$, $p = 0.165$).

TA – CA1

Only a small number of experiments were identified as having a TA component based on the presence of a long latency negativity at a spatial location at or just dorsal to the maximum amplitude of spontaneous theta/SO and also located above any other existing component of the PP response (either LPP or MPP). Using these criteria, only five experiments showed a distinguishable TA component. Single channel EPs containing this component, were similar to those previously described, having an average latency to peak negativity of 6.46 ± 0.33 ms and also demonstrating paired pulse facilitation (126 ± 4.6 percent) (Canning et al. 2000; Leung et al. 1995; Schall et al. 2007).

The average normalized (to theta) CSD sink values for TA stimulation in CA1 were 112.63 ± 6.56 for SO ($n = 5$), 80.26 ± 13.33 for the agonist condition ($n = 3$) and 119.62 ± 20.89 the antagonist condition (figure 3-8). Although the average sink values exhibited a high degree of variability the means follow the trend that would be expected in the TA with sinks being larger in SO than theta, decreasing after the injection of cholinergic agonists and increasing following the application of cholinergic antagonists.

Statistical analysis of the TA data was not carried out as sample sizes were to small for meaningful comparisons ($n < 5$).

Discussion

In addition to confirming our previous findings that hippocampal state influences synaptic excitability as a function of hippocampal subregion (Schall et al. 2007) the results of the current study propose that these effects are mediated by both direct and indirect cholinergic modulation. Consistent with our earlier study we found that stimulation of CA3 and TA inputs to CA1 as well as stimulation of LPP inputs to the DG produced significantly larger responses during SO while stimulation of MPP inputs to the DG yielded larger responses in theta. In parallel, following the application of a cholinergic agonist that elicited theta we found that responses to CA3, TA and LPP stimulation were reduced while MPP responses were enhanced. Likewise, application of muscarinic receptor antagonists that elicited SO activity produced an enhancement of synaptic excitability to CA3, TA and LPP stimulation while producing a reduced response to MPP stimulation.

Cholinergic and state modulation, implications for HPC processing:

Network state in the HPC during both sleep and urethane anesthesia is regulated primarily by cholinergic mechanisms, presumably arising from the medial septal region (Bland 1986; Wolansky et al. 2006). Our present results are consistent with this as both cholinergic agonism and antagonism abolished the spontaneous alternations of state that are typical of urethane anesthesia (Clement et al. 2006; Dickson et al. 2007). Our results,

in terms of synaptic excitability following cholinergic manipulations were consistent with a state-specific influence of synaptic modulation in each pathway studied. However, this modulation was often above and beyond what was expected for state itself, suggesting that cholinergic manipulations might have an additional effect on hippocampal synaptic excitability independent of state or that the cholinergic state was supranormal to the spontaneous one.

Our experimental procedure did not allow us to form conclusions as to whether the additional effects seen under cholinergic manipulation were due to changes in the influences of cholinergic projections to the HPC or produced through direct action on receptors in the hippocampal synapses themselves. It is conceivable that the theta and SO states produced under cholinergic conditions where altered compared to the natural states along some dimension that lead to changes in the synaptic responses. In fact for both theta and SO activity, the cholinergically induced states tended to have lower frequency bandwidths than their spontaneous counterparts. Since the frequency defined rhythms of theta and SO exert differential influences on synaptic excitability is seems reasonable to expect that other shifts in activity frequency would modulate excitability accordingly. In addition, it has been shown that synaptic excitability can be modified in hippocampal slices by the induction of a "theta-like" state following the application of a cholinergic agonist (Huerta and Lisman 1993). However, a number of hippocampal slice studies have conversely shown that the application of cholinergic agonists or antagonists produce effects on synaptic activity in the absence of state influences (Nakajima et al. 1986; Qian and Saggau 1997; Colgin et al. 2003). Further investigation beyond our results would be required to determine the exact nature of the enhanced cholinergic

modulation of hippocampal excitability but it seems likely to be explained by an interaction of both direct and indirect effects.

State and cholinergic modulation - Implications for behavior:

Further evidence for strong cholinergic link to hippocampal processing and synaptic activity may be taken from studies showing enhancement on memory tasks following the application of cholinergic agonists (Levin et al. 1996; Eidi et al. 2003) or impairments following the application of cholinergic antagonists (Givens and Olton 1990; Andersen et al. 2002). These results imply that cholinergically driven theta is essential for the proper functioning of learning and memory, as boosting theta leads to better performance while learning and retention abilities are decreased by its absence. Although the effects of cholinergic agonists and antagonists on memory performance are associated with the facilitation or disruption of the theta rhythm, it is not a far stretch to anticipate that their administration is ultimately influencing synaptic excitability in the HPC. Previous research has already established a link between cholinergic activity and hippocampal processing and our study further supports a relationship between the two. Our results indicate that alternations in state wield a large influence over synaptic excitability in the HPC and that this influence is adequately explained by cholinergic modulation. In fact it appears that cholinergic manipulations can enhance (or suppress) the excitability on hippocampal synapses beyond their normal standards. Thus understanding how normal state changes modify hippocampal processing in conjunction with how cholinergic manipulations can alter this processing could have broader implications for understanding and treating memory impairments.

Figure 3-1. Summary of Histological Placements. A) The dashed lines indicate probe placement and the dots indicate stimulating locations for CA3-CA1 experiments. B) The dashed lines indicate probe placement and the dots indicate stimulating locations for PP-DG experiments (green dots represent MPP only, blue dots represent LPP only and yellow dots represent both).

Figure 3-1

A. CA3 - CA1

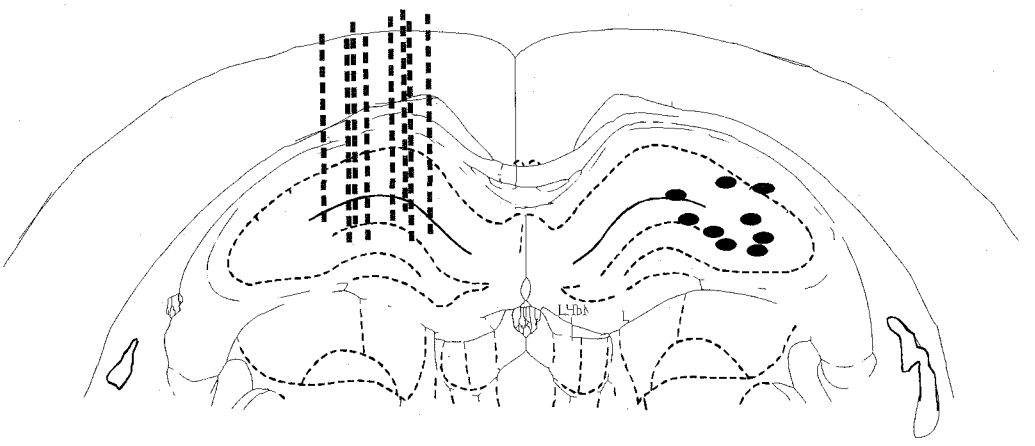

B. PP - DG

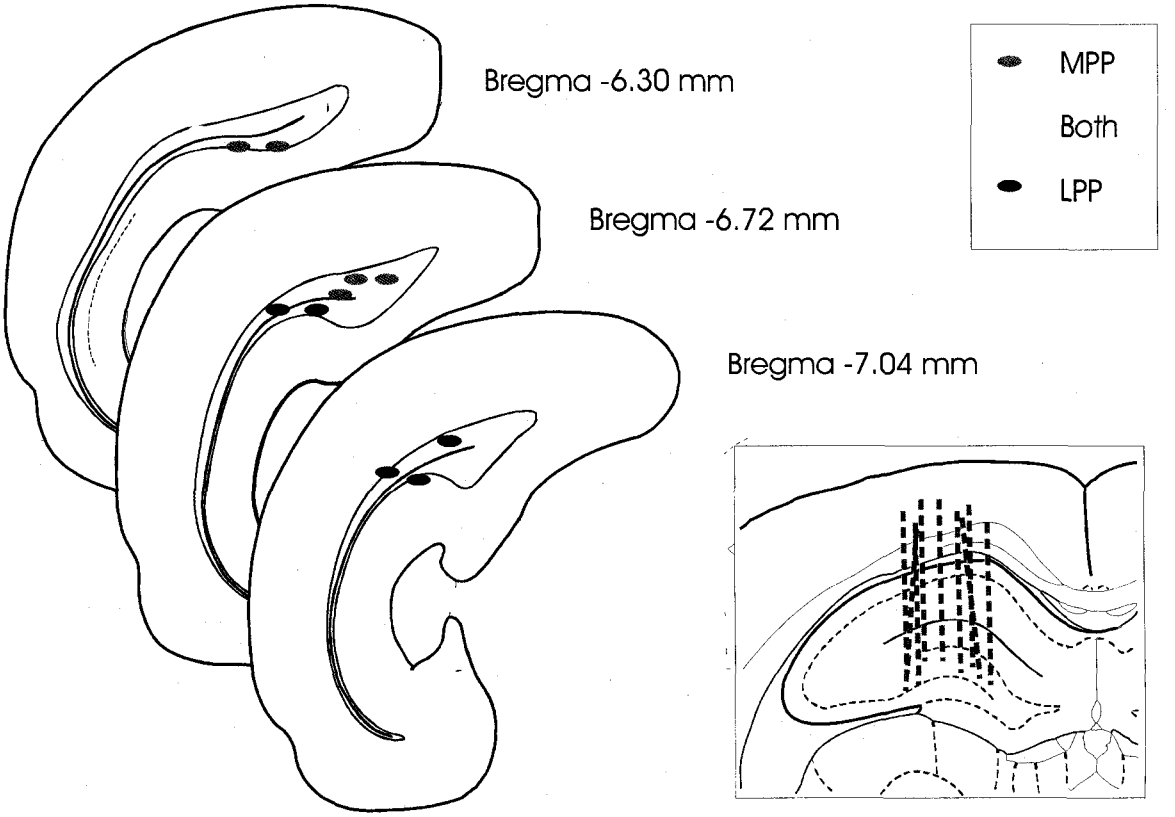

Figure 3-2. Spontaneous and Cholinergic States under Urethane Anesthesia. A) Raw traces of EEG activity taken during spontaneous theta, spontaneous SO, following the application of a cholinergic agonist and following the application of a cholinergic antagonist. Activity following the cholinergic agonist was similar to the spontaneous theta activity while activity following the cholinergic antagonist resembled spontaneous SO. B) The power spectrums of each of the four traces with spontaneous theta and SO superimposed and the cholinergically induced theta and SO superimposed for comparison.

Figure 3-2

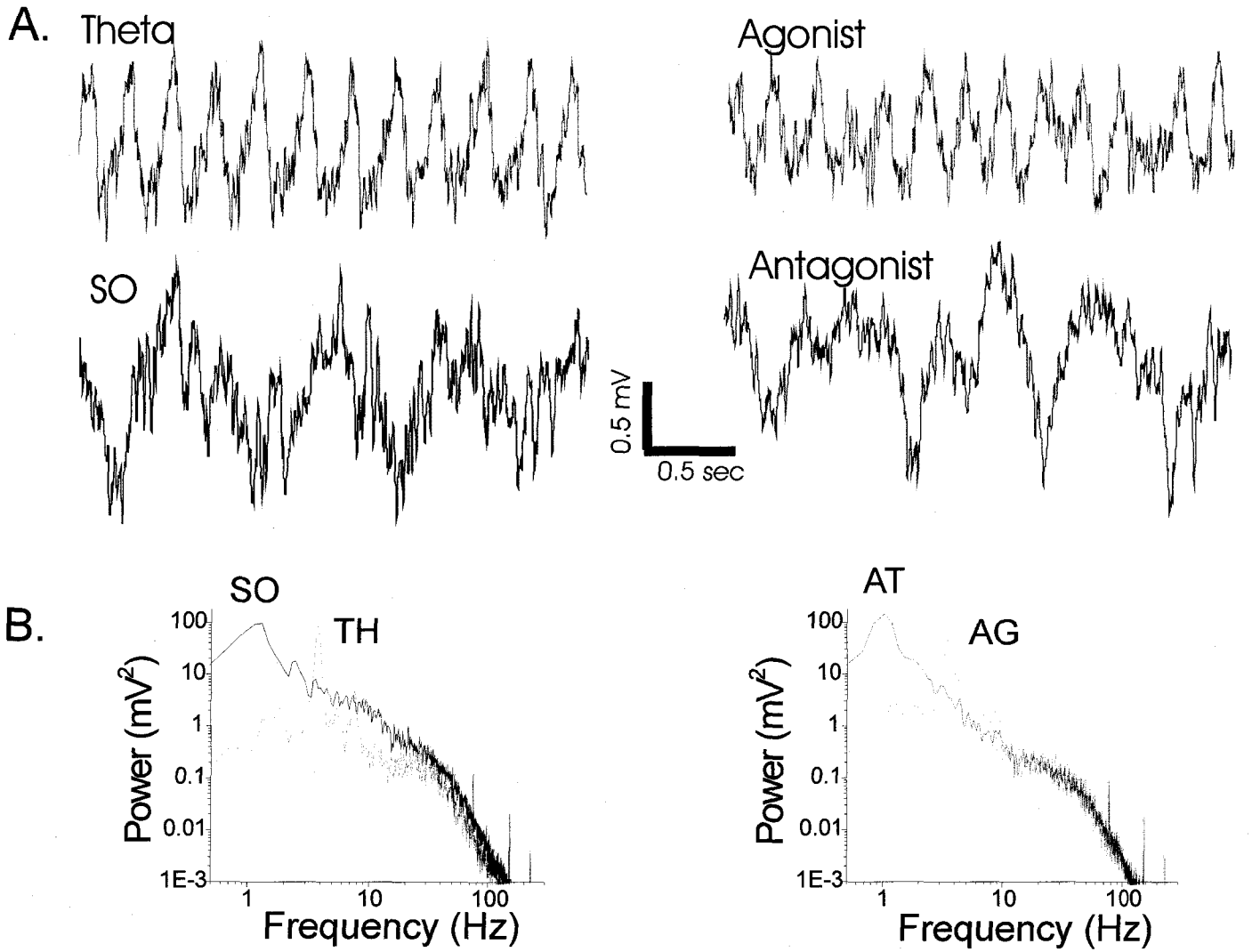
A.
Theta
SO
Agonist
Antagonist
0.5 mV
0.5 sec
B.
SO
TH
AT
AG
Power (mV²)
100
10
1
0.1
0.01
1E-3
1
10
100
Frequency (Hz)

Figure 3-3. Current Source Density (CSD) in CA1. A 16 contact multi-probe was lowered into the area CA1 of the hippocampus. A) From a continuous recording of spontaneous activity, samples of theta and SO were obtained and analyzed. Theta and SO profiles were constructed and used to help determine the level of the sink through identification of the theta reversal (in Stratum Radiatum) and the point of maximal theta (at the hippocampal fissure). The profiles show that the sink from the CSD plots in B is located above the hippocampal fissure in Stratum Radiatum. B) The CSD plots for this experiment were constructed by taking the average of 16 evoked potential profiles during spontaneous theta and SO activity as well as following the application of the cholinergic agonist and antagonist. The sink values from each condition indicated that the sink was larger during SO than theta, decreased after the agonist and increased following the antagonist.

Figure 3-3

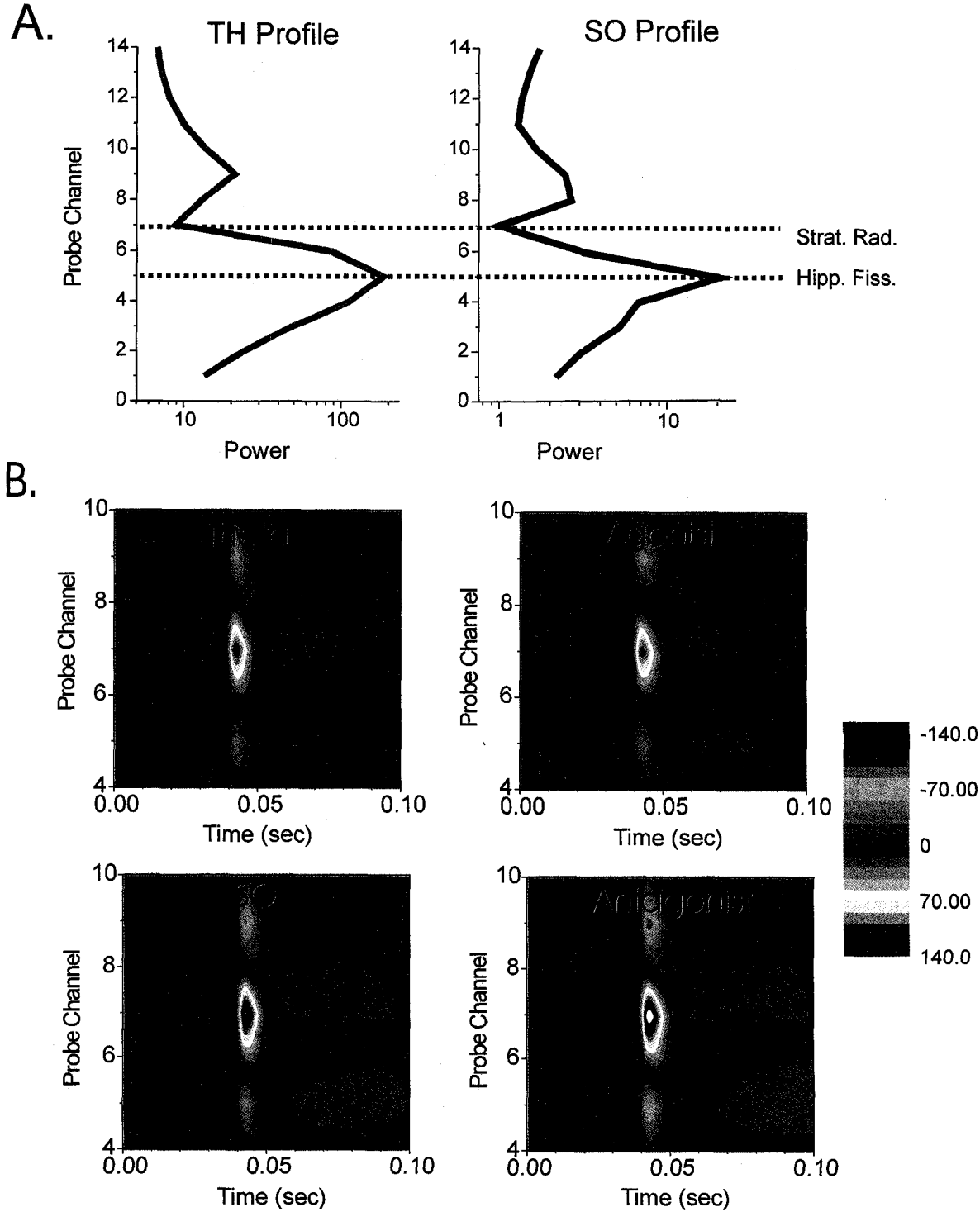
A.
TH Profile
SO Profile
Probe Channel
Power
Strat. Rad.
Hipp. Fiss.
B.
Probe Channel
Time (sec)
-140.0
-70.00
0
70.00
140.0

Figure 4. Spontaneous and Cholinergic State Means in CA1. Current sink values from the CSD plots were standardized within experiments then averaged across experiments and plotted. In CA1 sinks were larger during SO than theta, decreased in size following application of the cholinergic agonist and increased in size following the application of the cholinergic antagonist. The effects of the cholinergically induced theta state on synaptic excitability was in excess of that seen during spontaneous theta.

Figure 3-4

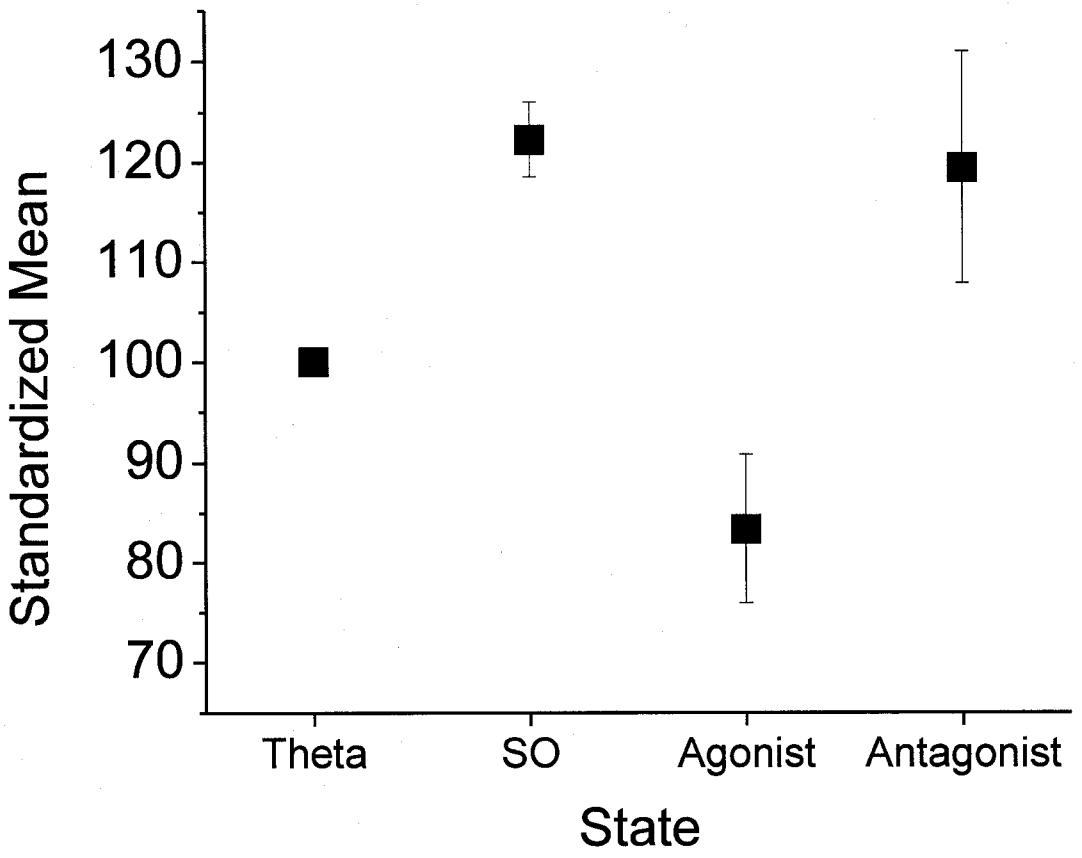
130
120
110
100
90
80
70
Standardized Mean
Theta
SO
Agonist
Antagonist
State

Figure 5. Current Source Density (CSD) for the MPP. A 16 contact multi-probe was lowered into the dentate gyrus of the hippocampus. A continuous recording of spontaneous activity was taken and samples of theta and SO were analyzed. Theta and SO profiles were constructed and used to help determine the level of the sink through identification of the theta reversal (in Stratum Radiatum) and the point of maximal theta (at the hippocampal fissure). The theta profiles for A) the experiment shown in C and B) the experiment shown in D are displayed, both showing the sinks are located below the hippocampal fissure in the molecular layer of the DG. C) The CSD plots for this experiment were constructed by taking the average of 16 EP profiles during spontaneous theta and SO activity as well as following the application of the cholinergic agonist (an antagonist sample was not obtained in this experiment). The sink values from each of the conditions indicate that the sink was larger during theta and increased in size following the application of the cholinergic agonist. D) The CSD plots for this experiment were constructed by taking the average of 16 EP profiles during spontaneous theta and SO activity as well as following the application of the cholinergic antagonist (an agonist sample was not obtained in this experiment). The sink values from each of the conditions show that the sink was larger in theta than SO and decreased in sized after injection of the cholinergic antagonist.

Figure 3-5

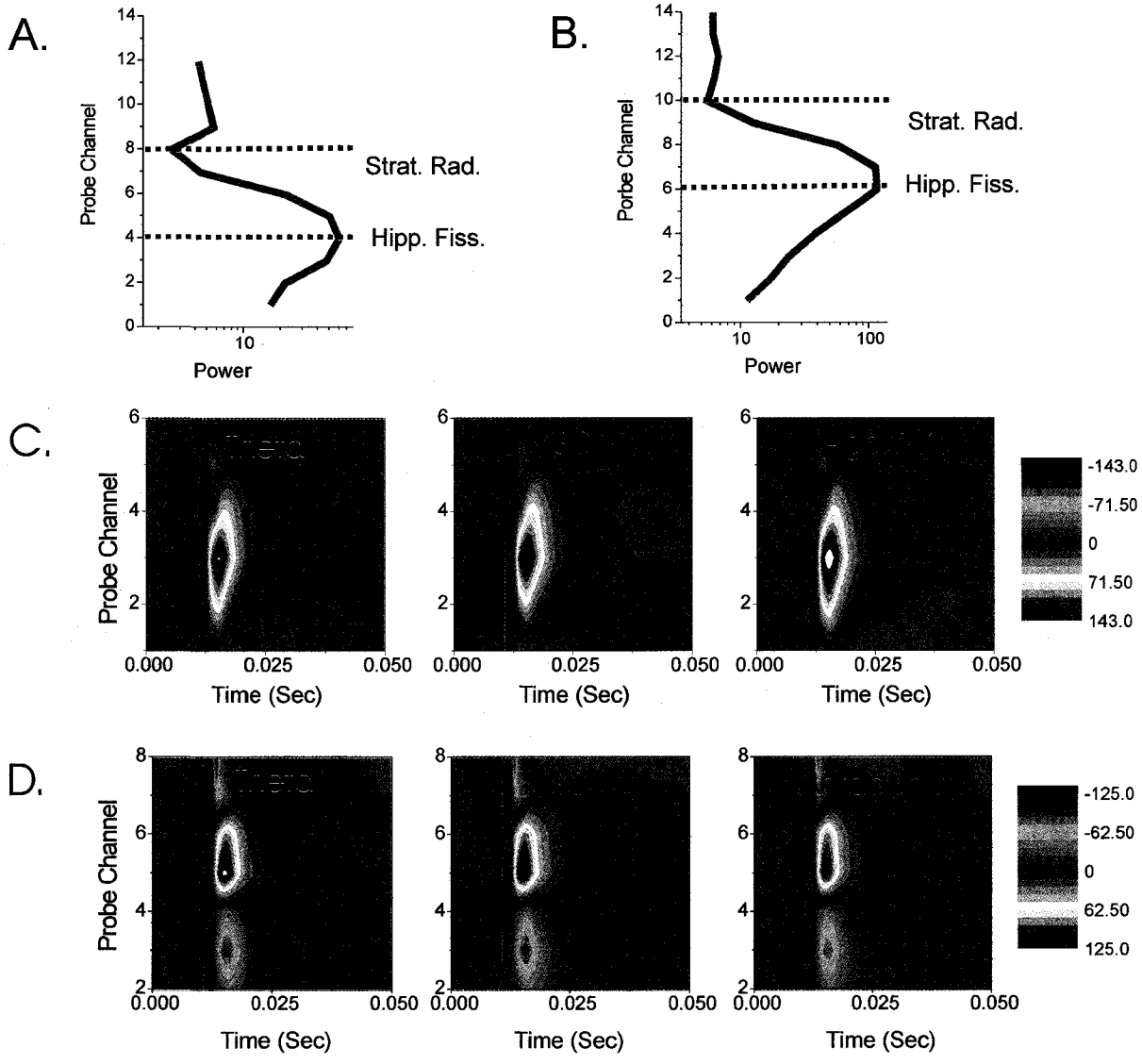
A.
Probe Channel
Strat. Rad.
Hipp. Fiss.
Power
B.
Porbe Channel
Strat. Rad.
Hipp. Fiss.
Power
C.
Probe Channel
Time (Sec)
-143.0
-71.50
0
71.50
143.0
D.
Probe Channel
Time (Sec)
-125.0
-62.50
0
62.50
125.0

Figure 6. Current Source Density (CSD) for the LPP. A 16 contact multi-probe was lowered into the dentate gyrus of the hippocampus. A) From a continuous recording of spontaneous activity, samples of theta and SO were obtained and analyzed. Theta and SO profiles were constructed and used to help determine the level of the sink through identification of the theta reversal (in Stratum Radiatum) and the point of maximal theta (at the hippocampal fissure). The profiles show that the sink from the CSD plots in B is located just below the hippocampal fissure in the molecular layer of the DG. B) The CSD plots for this experiment were constructed by taking the average of 16 EP profiles during spontaneous theta and SO activity as well as following the application of the cholinergic agonist and antagonist. The sink values from each of the conditions showed that sinks were larger during SO, decreased following injection of the cholinergic agonist and increased after the cholinergic antagonist.

Figure 3-6

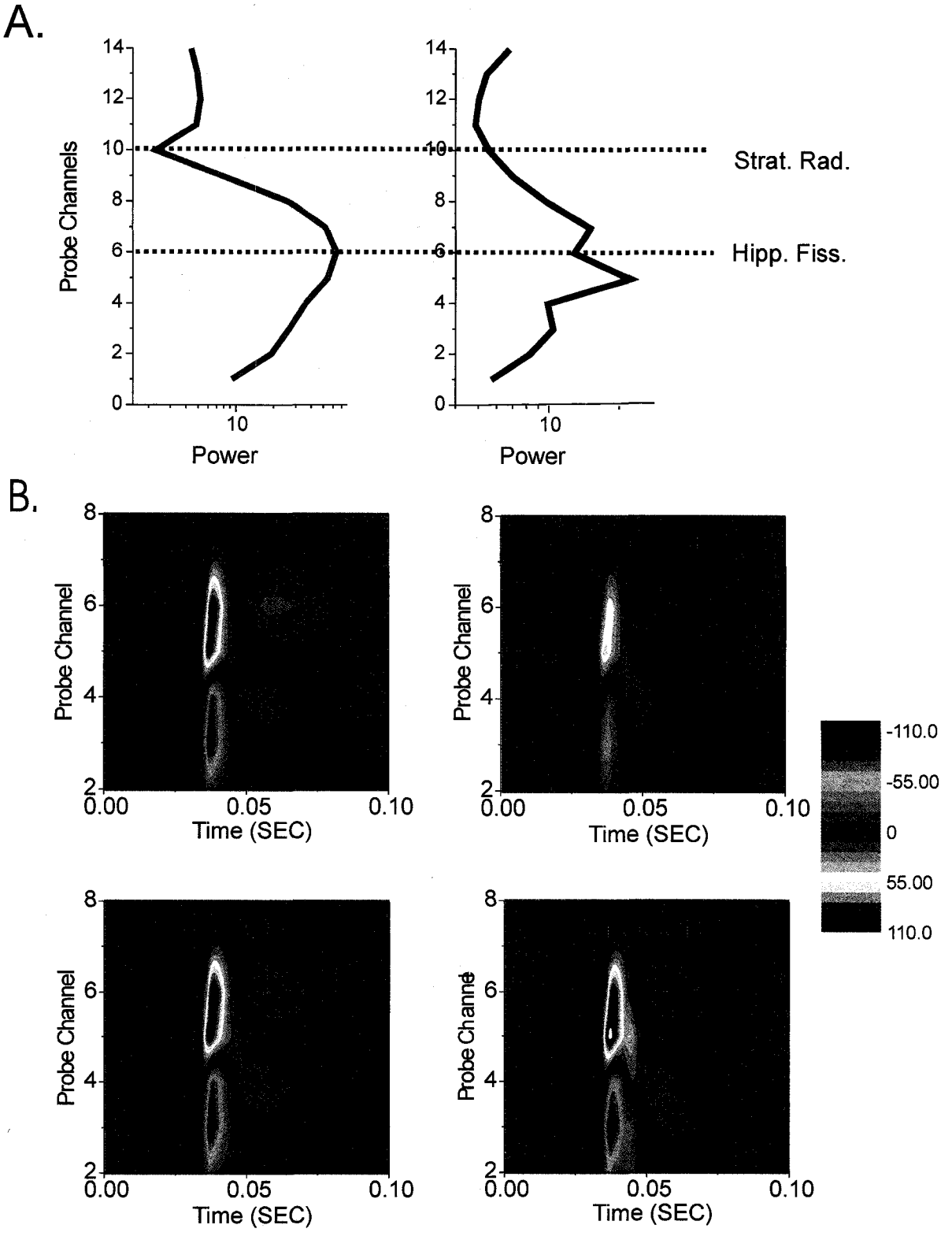
A.
Probe Channels
14
12
10
8
6
4
2
0
10
Power
Strat. Rad.
Hipp. Fiss.
B.
Probe Channel
8
6
4
2
0.00
0.05
0.10
Time (SEC)
-110.0
-55.00
0
55.00
110.0

Figure 7. Spontaneous and Cholinergic State Means for the MPP and LPP. Current sink values from the CSD plots were standardized within experiments then averaged across experiments and plotted. A) The MPP showed the opposite trend of CA1 where the average sink was larger in theta than SO, increased following the agonists and decreased after antagonist application. B) Results from the LPP were reversed from the MPP but in line with the results from CA1. In the LPP the average sink was larger in SO, became smaller following the cholinergic agonist and increased in size after the antagonist. In both the MPP and LPP, cholinergic states produced excitability responses beyond that observed during spontaneous states.

Figure 3-7

A.

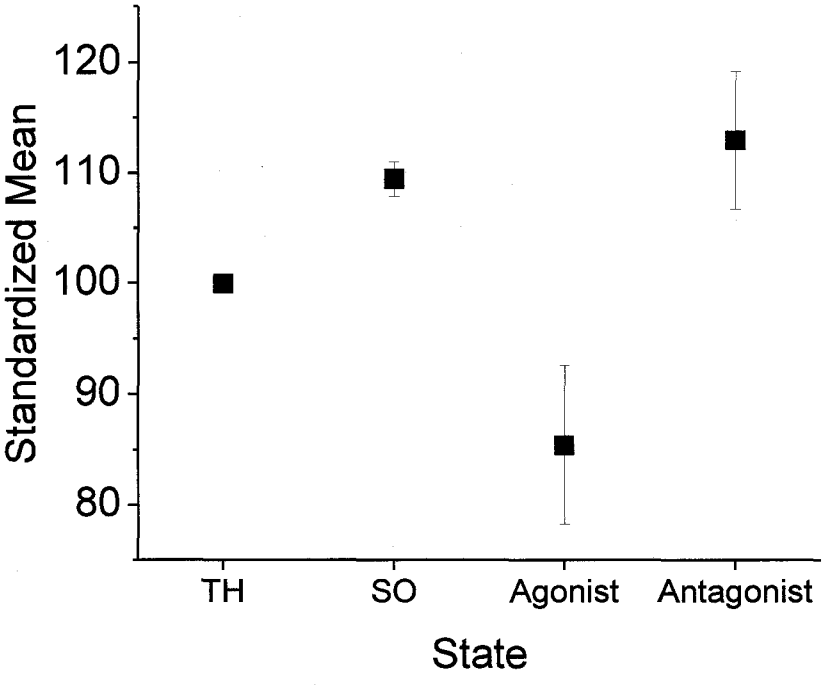
120
110
100
90
80
Standardized Mean
TH
SO
Agonist
Antagonist
State

B.

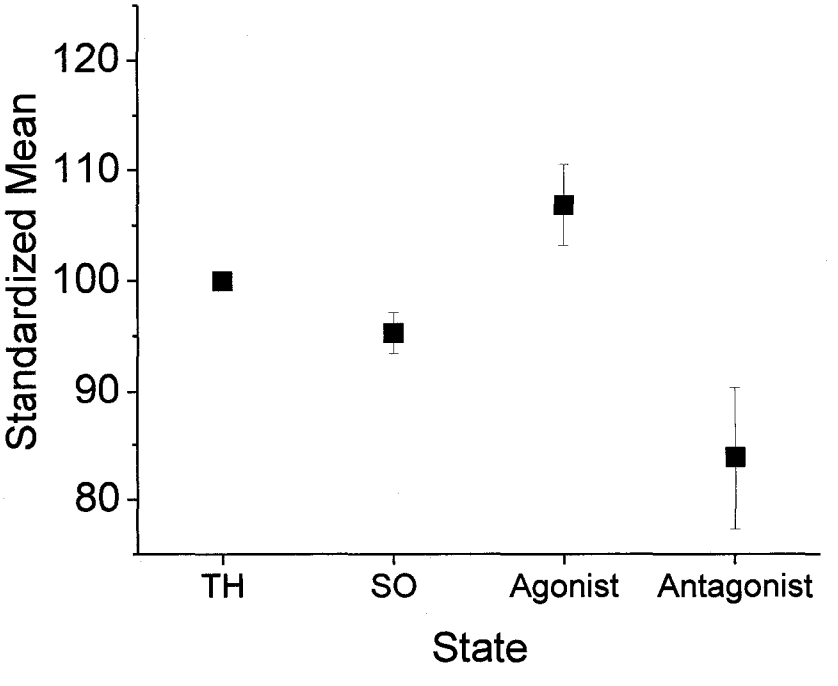
120
110
100
90
80
Standardized Mean
TH
SO
Agonist
Antagonist
State

Figure 8. Spontaneous and Cholinergic State Means for TA. Current sink values from the CSD plots were standardized within experiments then averaged across experiments and plotted. Although the results in TA exhibited a wide degree of variability they followed the same trend of commissural stimulated responses in CA1, as expected. Sinks were larger during SO, became reduced following cholinergic agonists and were enhanced following the cholinergic antagonist. However, sample sizes were too small ($n<5$) to conduct meaningful comparisons.

Figure 3-8

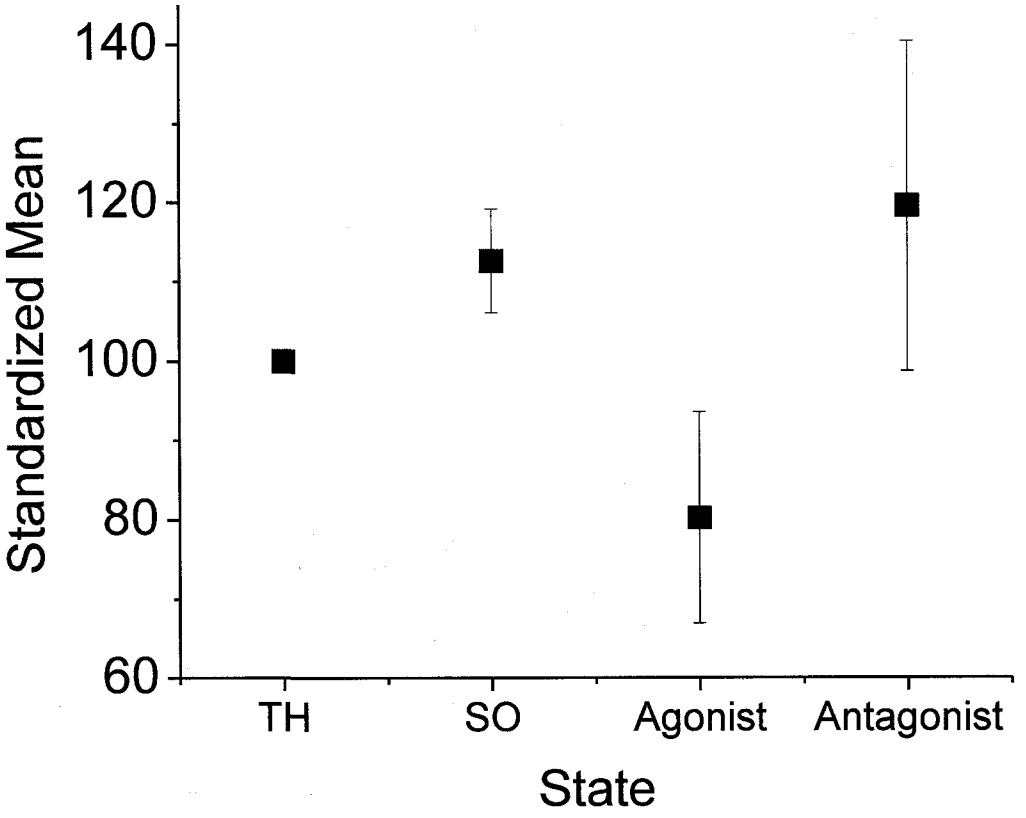
140
120
100
80
60
Standardized Mean
TH
SO
Agonist
Antagonist
State

References

Andersen JM, Lindberg V, and Myhrer T. Effects of scopolamine and D-cycloserine on non-spatial reference memory in rats. *Behavioural brain research* 129: 211-216, 2002.

Bland BH. The physiology and pharmacology of hippocampal formation theta rhythms. *Prog Neurobiol* 26: 1-54, 1986.

Bland SK, and Bland BH. Medial septal modulation of hippocampal theta cell discharges. *Brain research* 375: 102-116, 1986.

Buzsáki G. Two-stage model of memory trace formation: A role for "noisy" brain states. *Neurosci* 31: 551-570, 1989.

Buzsáki G, Grastyan E, Czopf J, Kellenyi L, and Prohaska O. Changes in neuronal transmission in the rat hippocampus during behavior. *Brain research* 225: 235-247, 1981.

Canning KJ, Wu K, Peloquin P, Kloosterman F, and Leung LS. Physiology of the entorhinal and perirhinal projections to the hippocampus studied by current source density analysis. *Ann N Y Acad Sci* 911: 55-72, 2000.

Clement E, Thwaites M, Richard A, Ailon J, Peters S, and Dickson C. Sleep-like rhythmic alternations of brain state under urethane anesthesia. In: *Soc Neurosci Abstracts*Society for Neuroscience, 2006, p. Program # 361.361.

Colgin LL, Kramar EA, Gall CM, and Lynch G. Septal modulation of excitatory transmission in hippocampus. *Journal of neurophysiology* 90: 2358-2366, 2003.

Dickson C, Lo A, Clement E, Mah E, and Richard A. Cyclical and sleep-like alternations of brain state are specific to urethane anaesthesia. In: *Society for Neuroscience Abstracts*2007, p. Program #791.793.

Eichenbaum H. Hippocampus: cognitive processes and neural representations that underlie declarative memory. *Neuron* 44: 109-120, 2004.

Eidi M, Zarrindast MR, Eidi A, Oryan S, and Parivar K. Effects of histamine and cholinergic systems on memory retention of passive avoidance learning in rats. *European journal of pharmacology* 465: 91-96, 2003.

Givens BS, and Olton DS. Cholinergic and GABAergic modulation of medial septal area: effect on working memory. *Behavioral neuroscience* 104: 849-855, 1990.

Huerta PT, and Lisman JE. Heightened synaptic plasticity of hippocampal CA1 neurones during a cholinergically induced rhythmic state. *Nature* 364: 723-725, 1993.

Leung LS. Behavior-dependent evoked potentials in the hippocampal CA1 region of the rat. I. Correlation with behavior and EEG. *Brain research* 198: 95-117, 1980.

Leung LS, Roth L, and Canning KJ. Entorhinal inputs to hippocampal CA1 and dentate gyrus in the rat: a current-source-density study. *Journal of neurophysiology* 73: 2392-2403, 1995.

Leung LW. Spectral analysis of hippocampal EEG in the freely moving rat: effects of centrally active drugs and relations to evoked potentials. *Electroencephalogr Clin Neurophysiol* 60: 65-77, 1985.

Levin ED, Kim P, and Meray R. Chronic nicotine working and reference memory effects in the 16-arm radial maze: interactions with D1 agonist and antagonist drugs. *Psychopharmacology* 127: 25-30, 1996.

Nakajima Y, Nakajima S, Leonard RJ, and Yamaguchi K. Acetylcholine raises excitability by inhibiting the fast transient potassium current in cultured hippocampal neurons. *Proceedings of the National Academy of Sciences of the United States of America* 83: 3022-3026, 1986.

Plihal W, and Born J. Effects of early and late nocturnal sleep on declarative and procedural memory. *J Cogn Neurosci* 9: 534–547., 1997.

Qian J, and Saggau P. Presynaptic inhibition of synaptic transmission in the rat hippocampus by activation of muscarinic receptors: involvement of presynaptic calcium influx. *British journal of pharmacology* 122: 511-519, 1997.

Schall KP, Kerber J, and Dickson CT. Rhythmic constraints on hippocampal processing: State and phase-related fluctuations of synaptic excitability during theta and the slow oscillation. *Journal of neurophysiology* 2007.

Scoville WB, and Milner B. Loss of recent memory after bilateral hippocampal lesions. *J Neurol Neurosurg Psychiat* 20: 11-21, 1957.

Segal M. A correlation between hippocampal responses to interhemispheric stimulation, hippocampal slow rhythmic activity and behaviour. *Electroencephalogr Clin Neurophysiol* 45: 409-411, 1978.

Squire LR. Memory and the hippocampus: a synthesis from findings with rats, monkeys, and humans. *Psychol Rev* 99: 195-231, 1992.

Stickgold R. Sleep-dependent memory consolidation. *Nature* 437: 1272-1278, 2005.

Vanderwolf CH. Cerebral activity and behavior: control by central cholinergic and serotoninergic systems. *Int Rev Neurobiol* 30: 225-340, 1988.

Wolansky T, Clement EA, Peters SR, Palczak MA, and Dickson CT. The hippocampal slow oscillation: A novel EEG state and its coordination with ongoing neocortical activity. *J Neurosci* 26: 6213-6229, 2006.

Wyble BP, Linster C, and Hasselmo ME. Size of CA1-evoked synaptic potentials is related to theta rhythm phase in rat hippocampus. *Journal of neurophysiology* 83: 2138-2144, 2000.

Chapter 4: Conclusions

In our experiments we found that all synaptic pathways in the HPC exhibited the tendency to modulate their responses across and within the rhythmic states of theta and SO as expressed under urethane anesthesia. More importantly, this modulation was differentially expressed in different pathways. The MPP demonstrated its highest excitability during theta, while all others, including the LPP, TA and commissural CA3-CA1 pathways, demonstrated their highest excitability during SO. It was notable, however, that the degree of modulation also appeared to be pathway dependent as well. Pathways terminating in the CA1 region (commissural and TA) demonstrated consistently larger differences between the theta and SO states whereas differential responses in the DG (MPP and LPP) were substantially lower and less consistently expressed. However, we confirmed that significant changes did exist in terms of synaptic (inward) current flow in all pathways which indicate increases or decreases in the degree of excitatory transmission via either pre- or post-synaptic mechanisms including neurotransmitter release, receptor activation, or both. In addition, we confirmed that this modulation appears to be dependent on central cholinergic mechanisms which could occur via indirect actions on forebrain state itself but also via direct actions within the hippocampus. At a minimum, these findings represent significant changes in the neural processing characteristics of the hippocampus as a function of state and thus have implications for hippocampal processing during alternations of brain state such as those occurring during sleep.

CA1, the Slow Oscillation and Consolidation

The largest effects of state on synaptic excitability occurred in CA1 where stimulation during SO produced significantly larger responses than theta or LIA. Traditionally studies on hippocampal activity have focused on theta, labeling it as the "activated" state while periods characterized by non-theta activity were considered "deactivated" states. The link between theta and synaptic plasticity (and consequently memory processes) has been extensively studied, especially in terms of LTP induction. Theta was first speculated as "the mechanism underlying memory" following the discovery that synapses in the HPC were potentiated most efficiently through simple stimulation patterns involving two events coinciding to the frequency of theta (Larson and Lynch 1986). Additional evidence for the importance of theta in hippocampal operations came from studies showing enhanced LTP after TBS stimulation (Hernandez et al. 2005) and differential influences of stimulation timed to the peaks and troughs of the ongoing theta rhythm (Hyman et al. 2003). These findings have led to the premise that theta is important for memory while other states in the HPC serve as baseline or resting periods. If theta is indeed the driving force behind the memory functions of the HPC the question emerges as to why any hippocampal synapse would be more excitable during a "deactivated" state?

A possible explanation to the potential contradiction comes from two recent lines of discovery. First of all, it has become evident that sleep plays a role in the proper functioning of memory. Recent studies have shown that manipulating a subject's REM sleep can influence their retention of procedural memories while manipulating their slow wave sleep produces effects on declarative memory recall (Plihal and Born 1997; Tucker

et al. 2006; Hornung et al. 2007). In one study, increasing the amount and stability of slow wave sleep in subjects through experimental manipulations lead to enhanced consolidation (Marshall et al. 2006), further implicating SO in the process of consolidating declarative, i.e. hippocampal dependent, memories. Secondly, it was recently brought to attention that the HPC is capable of engaging in slow wave activity, similar to that already known to occur in the cortex, during sleep and under urethane (Wolansky et al. 2006). Before the discovery of SO in the HPC it was believed that the HPC was only capable of LIA activity during cortical slow wave states. Importantly it was found that not only was the HPC exhibiting slow wave activity but that this activity could become correlated or synchronous with the slow wave activity observed in the cortex (Wolansky et al. 2006), providing a potential mode of communication and neural plasticity between the two regions.

Summarizing what is known about the HPC and consolidation, our results from CA1 synapses become more meaningful and relevant to the overall processing of memory. The HPC is crucial for forming new memories but appears to send them to the cortex for permanent storage in a process called consolidation. As consolidation is marked by the transfer of information out of the HPC it only stands to reason that the output synapses of the HPC should be primarily involved. An increasing body of evidence implicates slow wave activity as an important factor in the proper consolidation of declarative memories and recent studies show that slow wave activity is correlated between the HPC and its intended targets in the neocortex (Wolansky et al. 2006). Therefore, if CA1 neurons are responsible for sending information back to the neocortex and communication between

the two zones is facilitated by slow wave activity, it would be beneficial for these synapses to be more excitable during the SO state than during theta.

Different Functions for the MPP and LPP

Possibly the most interesting finding from these experiments was the different and opposing effects of state alternations on the synaptic excitability of the MPP and LPP, the two branches of the main input pathway into the HPC. The MPP was more excitable during periods of theta while the LPP showed greater excitability during periods of SO, with LIA generally producing intermediate responses in both pathways. Although the MPP and LPP both synapse onto the DG region of the HPC and were once considered as a single input pathway, a continuing collection of studies have since emerged establishing differences between the two pathways in terms of anatomy and physiological properties (McNaughton and Barnes 1977); (Dahl and Sarvey 1989); (Rush et al. 2001); (Hargreaves et al. 2005), consequently suggesting the two could be responsible for separate or opposing roles.

The fact that MPP and LPP synapses respond in essentially the opposite manner to one and other during shifts of hippocampal activity states strongly suggests they are involved in different aspects of memory processing. These differences could relate to the type of information each path in responsible for processing or even separate functions in the overall formation and consolidation of memory. The MPP and LPP originate in the medial and lateral regions of the EC respectively, which receive input from separate areas of the sensory cortex (Amaral 2007). Thus processing in the MPP and LPP could reflect

different types of sensory information or even represent a distinction between semantic and episodic memory.

Alternatively, the differences obtained between the MPP and LPP may represent involvement in different processes altogether rather than the management of different types of information. Based on research linking the theta rhythm to successful learning (Berry and Thompson 1978; Givens and Olton 1990; Hasselmo 2005), the heightened responsiveness of the MPP during theta suggests this pathway could be especially important for encoding information. The LPP on the other hand could be responsible for another function such as retrieving or consolidating memories that have been recently formed by the HPC. The LPP processes olfactory and emotional (amygdala) information while the MPP receives input from the remaining sensory areas (i.e. visual, auditory) (Dahl and Sarvey 1989)). This particular divergence of information is somewhat interesting considering that olfactory cues and emotional state have strong links with memory retrieval. One could speculate that the information carried in the MPP could be more important for information integration or contextual encoding while the information transferred through the LPP is more related to situations of recall. Further support of different functional roles in the two branches are indicated by findings that separately lesioning the MPP and LPP cause different effects on the behavior of animals, with lesions to the MPP appearing to have more of an effect on learning (Myhrer 1988; Ferbinteanu et al. 1999).

More Modulation within State

Although state alternations provide a powerful means for differential processing, our results, in accordance with previous findings (Wyble et al. 2000), suggest that more detailed processing can occur within the rhythmic states of theta and SO. For both theta and SO, evoked potentials followed a gradient where potentials generated during the falling phase of the cycle tended to be larger while potentials generated on the rising phase were generally smaller. The largest responses for both states occurred in the middle of the falling phase indicating that the effect was not solely attributable to the amount of membrane depolarization as maximal depolarization occurs at the bottom of the falling phase, just before the cycle began to rise again. Changes in the excitability of the neurons across the phase of the cycle have huge implications in how they interact with other neurons within the HPC as well as inputs from other structures. The modulation of synaptic response across the phase of the cycle could have implications for input selection, synchronization of inputs and outputs or phase precision. It has even been suggested that the pattern of excitability produced during the phase cycles of the theta rhythm (i.e. differences between the peaks and troughs of the rhythm) could be responsible for determining periods of information encoding versus retrieval within the HPC (Hasselmo 2005).

Acetylcholine

Finally, our results indicate that the modulation of synaptic responses we observed were dependent on cholinergic activity in the HPC. The theta and SO activity observed during urethane anesthesia are regulated by cholinergic inputs, with cholinergic agonists

promoting theta and cholinergic antagonists promoting SO (Wolansky et al. 2006). We found that applying the cholinergic agonists oxotremorine or eserine lead to an extended theta state accompanied by a similar degree pattern of synaptic excitability in CA1, MPP, LPP and TA as compared to spontaneous theta while the application of the cholinergic agonists atropine or scopolamine produced a prolonged state of SO activity and a similar degree of synaptic excitability as compared to spontaneous SO. In many cases the application of cholinergic agonists or antagonist lead to synaptic responses that were beyond those seen under natural conditions indicating that either acetylcholine produces direct effects on the synaptic response separate from state influence or artificial cholinergic modulation alters theta and SO activity changing their influence on synaptic excitability. Further study as to whether the cholinergic effects we observed were due to an indirect effect on state, a direct effect on hippocampal receptors or a combination of the two could be beneficial as a means of understanding and combating memory disabilities. Spontaneous state alternations regulate a system of synaptic dynamics which control hippocampal processing and cholinergic agents were found to modulate these synaptic responses in excess of what was seen under natural conditions. As such, specific cholinergic manipulations, timed accordingly, could be applied to enhance the synaptic excitability of desired pathways and increase the transmission of information in an attempt offset decreased memory abilities produced by natural aging or diseases such as Alzheimer's.

One final consideration from our experiments is the use of urethane anesthesia and the ability to generalize our results. Obviously, results obtained from an animal under anesthesia are not directly comparable to what would be expected in an awake behaving

animal but there is evidence that the activity exhibited under urethane and during sleep is very similar (Clement et al. 2006). During both sleep and urethane rats cycle in a predictable manner through periods of theta, LIA and SO which is determined by cholinergic modulation in both cases (Clement et al. 2006). Thus it is reasonable to assume that the behavior of the synapses during theta, LIA and SO under urethane has implications for activity during natural sleep conditions. In addition, one might expect the general trends of state influence observed in the HPC under urethane to extend to behavior of the HPC in general, even during wakefulness, as supported by studies that have found state modulation of synaptic excitability in freely behaving rats (Leung 1980), including opposing trends of excitability in CA1 and the DG (Buzsáki et al. 1981). It would be interesting to properly confirm this by studying the differences in response patterns exhibited by the synapses of the MPP, LPP and CA1 in freely behaving rats. Nevertheless, we have shown significant modulation of synaptic response across alternations of state similar to those observed during sleep cycles which have become heavily associated to memory processing. Our results indicate that the HPC possesses the mechanisms, through an interaction of state and region, for a highly complex system of information processing. In addition, our particular pattern of results offer further support for the role of SO in consolidation of memories from the HPC to the neocortex, and to a lesser extent, the role of theta in memory formation.

References

Amaral DGL, P. Hippocampal Neuroanatomy. In: *The Hippocampus Book*, edited by Andersen P, Morris, R., Amaral, D., Bliss, T. & O'Keefe, J. New York, New York: Oxford University Press, Inc., 2007.

Berry SD, and Thompson RF. Prediction of learning rate from the hippocampal electroencephalogram. *Science (New York, NY* 200: 1298-1300, 1978.

Buzsáki G, Grastyan E, Czopf J, Kellenyi L, and Prohaska O. Changes in neuronal transmission in the rat hippocampus during behavior. *Brain research* 225: 235-247, 1981.

Clement E, Thwaites M, Richard A, Ailon J, Peters S, and Dickson C. Sleep-like rhythmic alternations of brain state under urethane anesthesia. In: *Soc Neurosci Abstracts*Society for Neuroscience, 2006, p. Program # 361.361.

Dahl D, and Sarvey JM. Norepinephrine induces pathway-specific long-lasting potentiation and depression in the hippocampal dentate gyrus. *Proceedings of the National Academy of Sciences of the United States of America* 86: 4776-4780, 1989.

Ferbinteanu J, Holsinger RM, and McDonald RJ. Lesions of the medial or lateral perforant path have different effects on hippocampal contributions to place learning and on fear conditioning to context. *Behavioural brain research* 101: 65-84, 1999.

Givens BS, and Olton DS. Cholinergic and GABAergic modulation of medial septal area: effect on working memory. *Behavioral neuroscience* 104: 849-855, 1990.

Hargreaves EL, Rao G, Lee I, and Knierim JJ. Major dissociation between medial and lateral entorhinal input to dorsal hippocampus. *Science (New York, NY* 308: 1792-1794, 2005.

Hasselmo ME. What is the function of hippocampal theta rhythm?--Linking behavioral data to phasic properties of field potential and unit recording data. *Hippocampus* 15: 936-949, 2005.

Hernandez RV, Navarro MM, Rodriguez WA, Martinez JL, Jr., and LeBaron RG. Differences in the magnitude of long-term potentiation produced by theta burst and high frequency stimulation protocols matched in stimulus number. *Brain Res Brain Res Protoc* 15: 6-13, 2005.

Hornung OP, Regen F, Warnstedt C, Anghelescu I, Danker-Hopfe H, Heuser I, and

Lammers CH. Declarative and procedural memory consolidation during sleep in patients with borderline personality disorder. *J Psychiatr Res* 2007.

Hyman JM, Wyble BP, Goyal V, Rossi CA, and Hasselmo ME. Stimulation in hippocampal region CA1 in behaving rats yields long-term potentiation when delivered to the peak of theta and long-term depression when delivered to the trough. *J Neurosci* 23: 11725-11731, 2003.

Larson J, and Lynch G. Induction of synaptic potentiation in hippocampus by patterned stimulation involves two events. *Science (New York, NY* 232: 985-988, 1986.

Leung LS. Behavior-dependent evoked potentials in the hippocampal CA1 region of the rat. I. Correlation with behavior and EEG. *Brain research* 198: 95-117, 1980.

Marshall L, Helgadottir H, Molle M, and Born J. Boosting slow oscillations during sleep potentiates memory. *Nature* 444: 610-613, 2006.

McNaughton BL, and Barnes CA. Physiological identification and analysis of dentate granule cell responses to stimulation of the medial and lateral perforant pathways in the rat. *The Journal of comparative neurology* 175: 439-454, 1977.

Myhrer T. Exploratory behavior and reaction to novelty in rats with hippocampal perforant path systems disrupted. *Behavioral neuroscience* 102: 356-362, 1988.

Plihal W, and Born J. Effects of early and late nocturnal sleep on declarative and procedural memory. *J Cogn Neurosci* 9: 534–547., 1997.

Rush AM, Rowan MJ, and Anwyl R. Application of N-methyl-D-aspartate induces long-term potentiation in the medial perforant path and long-term depression in the lateral perforant path of the rat dentate gyrus in vitro. *Neurosci Lett* 298: 175-178, 2001.

Tucker MA, Hirota Y, Wamsley EJ, Lau H, Chaklader A, and Fishbein W. A daytime nap containing solely non-REM sleep enhances declarative but not procedural memory. *Neurobiology of learning and memory* 86: 241-247, 2006.

Wolansky T, Clement EA, Peters SR, Palczak MA, and Dickson CT. The hippocampal slow oscillation: A novel EEG state and its coordination with ongoing neocortical activity. *J Neurosci* 26: 6213-6229, 2006.

Wyble BP, Linster C, and Hasselmo ME. Size of CA1-evoked synaptic potentials is related to theta rhythm phase in rat hippocampus. *Journal of neurophysiology* 83: 2138-2144, 2000.